2011

# NEW ACCURATE FAULT LOCATION ALGORITHM FOR PARALLEL TRANSMISSION LINES

Pramote Chaiwan
*University of Kentucky*, joechaiwan@yahoo.com

# NEW ACCURATE FAULT LOCATION ALGORITHM FOR PARALLEL TRANSMISSION LINES

DISSERTATION

A dissertation submitted in partial fulfillment of the requirements for the degree of Doctor of Philosophy in the College of Engineering at the University of Kentucky

By
Pramote Chaiwan

Lexington, Kentucky

Director: Dr. Yuan Liao, Professor of Electrical and Computer Engineering

Lexington, Kentucky

2011

ABSTRACT OF DISSERTATION

NEW ACCURATE FAULT LOCATION ALGORITHM FOR PARALLEL TRANSMISSION LINES

Electric power systems have been in existence for over a century. Electric power transmission line systems play an important role in carrying electrical power to customers everywhere. The number of transmission lines in power systems is increasing as global demand for power has increased. Parallel transmission lines are widely used in the modern transmission system for higher reliability. The parallel lines method has economic and environmental advantages over single circuit. A fault that occurs on a power transmission line will cause long outage time if the fault location is not located as quickly as possible. The faster the fault location is found, the sooner the system can be restored and outage time can be reduced.

The main focus of this research is to develop a new accurate fault location algorithm for parallel transmission lines to identify the fault location for long double-circuit transmission lines, taking into consideration mutual coupling impedance, mutual coupling admittance, and shunt capacitance of the line.

In this research, the equivalent PI circuit based on a distributed parameter line model for positive, negative, and zero sequence networks have been constructed for system analysis during the fault. The new method uses only the voltage and current from one end of parallel lines to calculate the fault distance. This research approaches the problem by derivation all equations from positive sequence, negative sequence, and zero sequence network by using KVL and KCL. Then, the fault location is obtained by solving these equations. EMTP has been utilized to generate fault cases under various fault conditions with different fault locations, fault types and fault resistances. Then the algorithm is evaluated using the simulated data. The results have shown that the developed algorithm can achieve highly accurate estimates and is promising for practical applications.

KEYWORDS: Distributed parameter line model, Parallel transmission line, Equivalent PI circuit, Mutual coupling impedance, Fault location

Pramote Chaiwan

Student's Signature

September 21, 2011

Date

# NEW ACCURATE FAULT LOCATION ALGORITHM FOR PARALLEL TRANSMISSION LINES

By

Pramote Chaiwan

Dr.Yuan Liao

Director of Dissertation

Dr. Zhi David Chen

Director of Graduate Studies

DEDICATION

This dissertation is dedicated to my parents

Mr. Dee Chaiwan

and

Mrs. Sumontha Chaiwan

ACKNOWLEDGMENTS

I am heartily thankful to my advisor, Dr. Yuan Liao, whose guidance, encouragement, and support from the initial to the final level enabled me to develop an understanding of this research. This dissertation would not have been possible without his help. I also would like to thank Dr. YuMing Zhang, Dr.Jimmie Cathey, and Dr. Alan Male for their support in a number of ways to serve on the Dissertation Advisory Committee. I would like to thank Dr. Zhongwei Shen of the MAT Program to serve as the Outside Examiner. It is my pleasure to thank the faculty members who made this dissertation possible. I also would like to thank my parents and family members, who have been waiting to see my success and my friends Anthony M. King and Sam tantasook for their support.

TABLE OF CONTENTS

LIST OF TABLES

LIST OF FIGURES

# CHAPTER ONE

## I. INTRODUCTION

Power transmission systems have been in existence for over a century. Power transmission systems play an important role in carrying electrical power to customers everywhere. The number of transmission lines in power systems is increasing as global demand for power has expanded. Currently, the bulk transmission of electrical power is done by means of parallel lines which are widely used in the modern transmission systems. The parallel lines method has economic and environmental advantages over single circuit. Unfortunately, a fault that occurs in one part of the power system, such as a generator or power transmission line, can destroy the whole system if the fault location is not located as quickly as possible. The faster the fault location is found, the sooner the system can be restored and outage time can be reduced.

The double-circuit transmission line is used more often than the single-circuit and the principle of distance relaying states that the impedance measured by a relay is proportional to the distance of that relay to the fault. Therefore, by measuring the impedance it can be determined whether the line being protected is faulted or not.

Unfortunately, there are several ways for the following to be errors in accurately measuring a fault location, and they should be taken into full consideration.

1. The self-impedance, mutual impedances and mutual admittance

The positive sequence mutual impedances and the negative-sequence mutual impedances are about 3-5% of its own self-impedances. The zero-sequence mutual impedances are about 50-55% of the zero-sequence self-impedances. Thus, the error occurs if the calculation of the fault location considers only the self-impedances.

2. Shunt capacitance

For long-length transmission lines (more than 150 miles or 240 km), the line is considered to have a shunt capacitance instead of lumped parameters for the calculation of exact fault location. If lumped parameters are used, then errors will occur.

3. Fault resistance

The fault resistance can only be determined using the algorithm that will be proposed in this dissertation. Therefore, it cannot be used as input to determine the fault location.

4. Source impedance

The changing of the source impedance without changing the setting of the fault calculation equipment can cause an error in the accurate calculation of fault location.

5. Capacitance voltage transformer

6. The classification of the transmission line

Lack of knowledge of the classification of transmission lines can lead to error in the calculation of the accurate fault location. There are

three classes of transmission lines: short, medium, and long transmission lines.

In the short-length line class (less than 50 miles or 80 km), the shunt capacitance is considered so small that can be ignored. We only consider the series of resistance R and inductance L.

In the medium-line class (50 to 150 miles or 80 to 240 km), the capacitance will be represented as two capacitors each equal to half the line capacitance, which is known as the nominal-π model.

In the long-length line class (more than 150 miles or 240 km), the line is considered to have distributed parameters instead of lumped parameters. This will provide accurate results. It is referred to as the equivalent-π model since it has lumped parameters which are adjusted so that they are equivalent to the exact distributed parameter model.

The purpose of this research is to improve the fault distance estimation for long parallel transmission lines, taking into consideration mutual coupling impedance and mutual coupling admittance. The distributed transmission line parameters model will be employed.

# II. BACKGROUND

In order to estimate the fault distance, the following concepts needs to be explained:

1. Symmetrical Component and Sequence Networks
2. Unsymmetrical Faults

## 1. Symmetrical Component and Sequence Networks

The well-known theory of symmetrical component that was introduced by Charles Legeyt Fortescue is very useful to solve the problems for unbalanced condition on power systems. According to his theory, unbalanced three phase faults can be resolved into three sets of balanced three phase systems by using the method of symmetrical components that consists of:

1.1 Positive sequence component, which consists of three phasors with equal magnitudes and 120° apart from each other, and phase sequence are the same as original phasors.

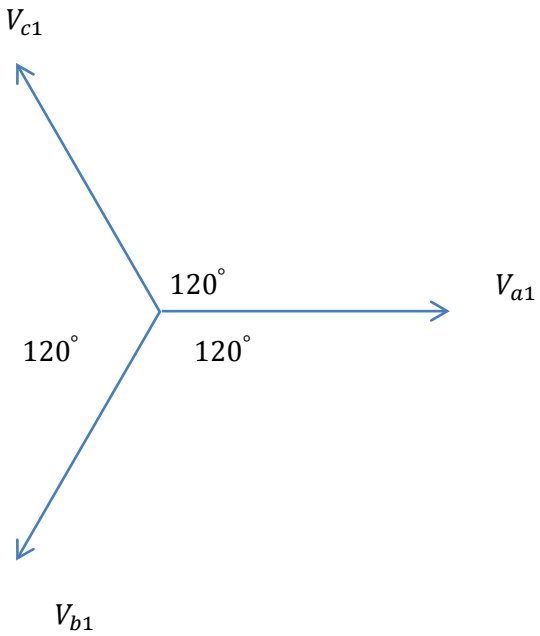


Figure1.1 Positive sequence component

1.2 Negative sequence component, which consists of three phasors with equal magnitudes and 120° apart from each other, and phase sequence are opposites of the original phasors.

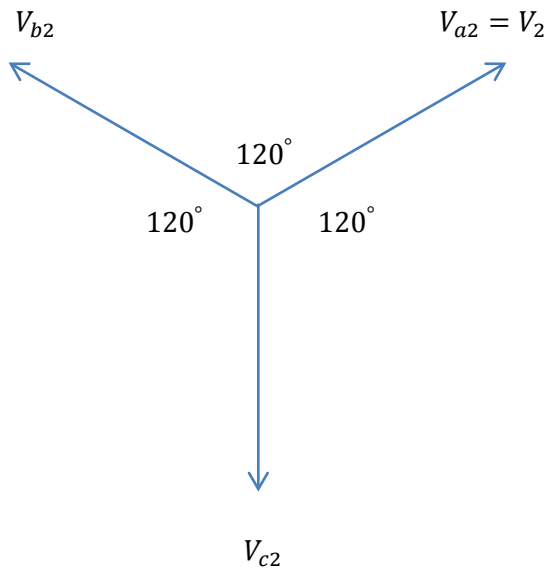


Figure 1.2 Negative sequence component

1.3 Zero sequence component, which consists of three phasors with equal magnitudes and zero phase displacements from each other.

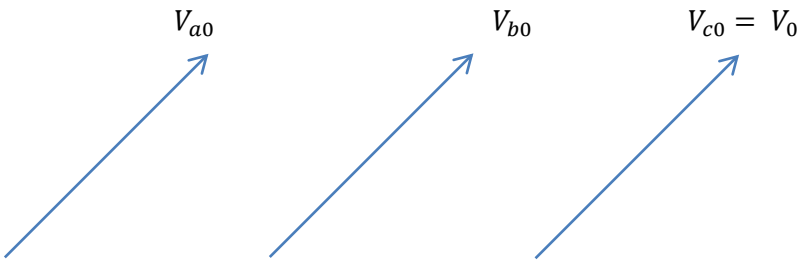


Figure 1.3 Zero sequence component

In the power system that consists of three phases such as a, b, and c

$$V_a = V_{a0} + V_{a1} + V_{a2}$$

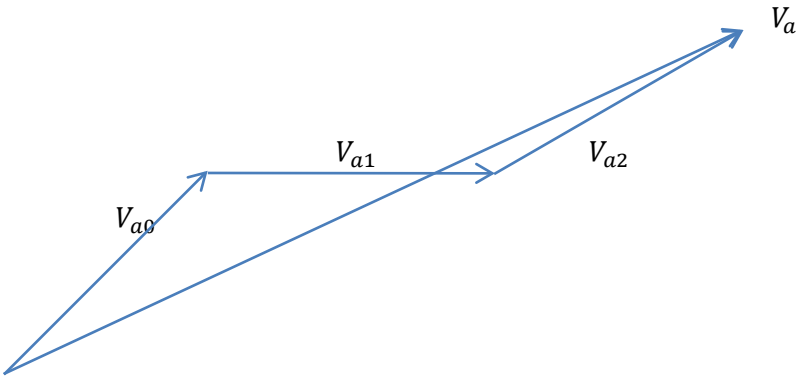


Figure 1.4 Components of phase a

$$V_b = V_{b0} + V_{b1} + V_{b2}$$

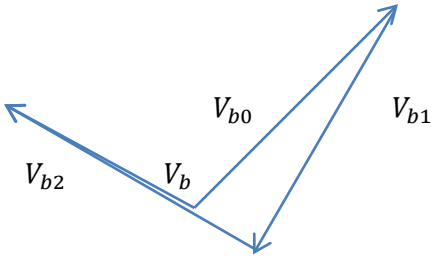


Figure 1.5 Components of Phase b

$$V_c = V_{c0} + V_{c1} + V_{c2}$$

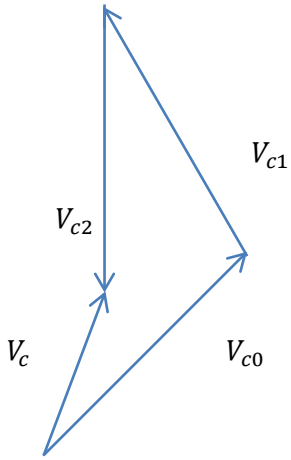


Figure 1.6 Components of phase c

Then phase a, b, and c can be obtained as follow:

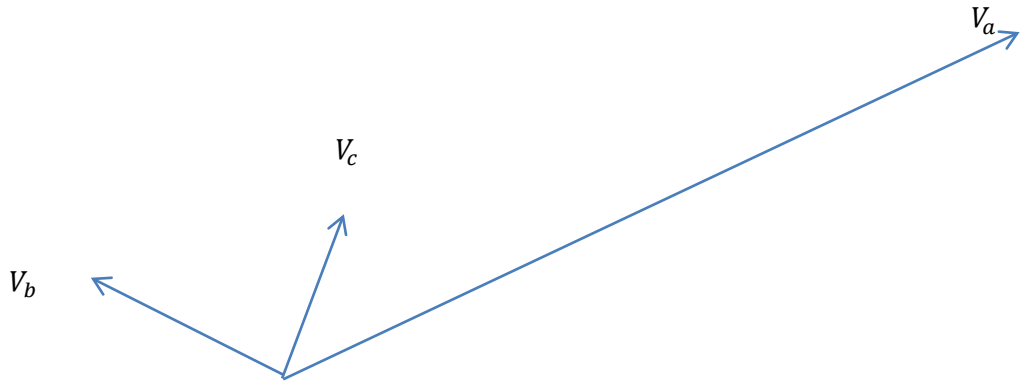


Figure 1.7 Three unbalanced phasors a, b, and c that were obtained from three set of balanced phasors

Where $a = 1\angle 120° = -0.5 + j0.866$ (1.1)

$a^2 = 1\angle 240° = -0.5 - j0.866$ (1.2)

$a^3 = 1\angle 360° = 1\angle 0° = 1.0 + j0$ (1.3)

$V_{b0} = V_{a0}$ (1.4)

$V_{b1} = a^2 V_{a1}$ (1.5)

$V_{b2} = aV_{a2}$ (1.6)

$V_{c0} = V_{a0}$ (1.7)

$V_{c1} = aV_{a1}$ (1.8)

$V_{c2} = a^2 V_{a2}$ (1.9)

Thus

$V_a = V_{a0} + V_{a1} + V_{a2}$ (1.10)

$$V_b = V_{a0} + a^2 V_{a1} + a V_{a2} \tag{1.11}$$

$$V_c = V_{a0} + a V_{a1} + a^2 V_{a2} \tag{1.12}$$

$$\begin{bmatrix} V_a \\ V_b \\ V_c \end{bmatrix} = \begin{bmatrix} 1 & 1 & 1 \\ 1 & a^2 & a \\ 1 & a & a^2 \end{bmatrix} \begin{bmatrix} V_{a0} \\ V_{a1} \\ V_{a2} \end{bmatrix} = A \begin{bmatrix} V_{a0} \\ V_{a1} \\ V_{a2} \end{bmatrix} \tag{1.13}$$

where

$$A = \begin{bmatrix} 1 & 1 & 1 \\ 1 & a^2 & a \\ 1 & a & a^2 \end{bmatrix} \tag{1.14}$$

Then

$$A^{-1} = \frac{1}{3} \begin{bmatrix} 1 & 1 & 1 \\ 1 & a & a^2 \\ 1 & a^2 & a \end{bmatrix} \tag{1.15}$$

$$\begin{bmatrix} V_{a0} \\ V_{a1} \\ V_{a2} \end{bmatrix} = \frac{1}{3} \begin{bmatrix} 1 & 1 & 1 \\ 1 & a & a^2 \\ 1 & a^2 & a \end{bmatrix} \begin{bmatrix} V_a \\ V_b \\ V_c \end{bmatrix} = A^{-1} \begin{bmatrix} V_a \\ V_b \\ V_c \end{bmatrix} \tag{1.16}$$

We have

$$V_{a0} = \frac{1}{3}(V_a + V_b + V_c) \tag{1.17}$$

$$V_{a1} = \frac{1}{3}(V_a + a V_b + a^2 V_c) \tag{1.18}$$

$$V_{a2} = \frac{1}{3}(V_a + a^2 V_b + a V_c) \tag{1.19}$$

For current we also have

$$I_a = I_{a0} + I_{a1} + I_{a2} \tag{1.20}$$

$$I_b = I_{a0} + a^2 I_{a1} + a I_{a2} \tag{1.21}$$

$$I_c = I_{a0} + a I_{a1} + a^2 I_{a2} \tag{1.22}$$

$$I_{a0} = \frac{1}{3}(I_a + I_b + I_c) \tag{1.23}$$

$$I_{a1} = \frac{1}{3}(I_a + a I_b + a^2 I_c) \tag{1.24}$$

$$I_{a2} = \frac{1}{3}(I_a + a^2 I_b + a I_c) \quad (1.25)$$

## 2. Unsymmetrical Faults

2.1 Unsymmetrical faults can be classified into:

2.1.1 Single line to ground fault: a-g, b-g, and c-g

2.1.2 Line to line faults: ab, bc, and ca

2.1.3 Double line to ground fault: abg, bcg, and cag

2.1.4 Three phase fault: abc

As the unbalanced fault occurs in the power system during the fault, the unbalanced current will go into the system. The method of symmetrical component will be utilized to calculate the current on the system.

2.2 Voltage and Current network equation in Sequence component

The voltages in electric power system are assumed to be balanced until the fault occurred. Only positive sequence component of the pre-fault voltage $V_f$ is considered.

$$V_0 = 0 - Z_0 I_{a0} \quad (1.26)$$

$$V_{a1} = E_f - Z_1 I_{a1} \quad (1.27)$$

$$V_{a2} = 0 - Z_2 I_{a2} \quad (1.28)$$

This can be written in the matrix form as

$$\begin{bmatrix} V_{a0} \\ V_{a1} \\ V_{a2} \end{bmatrix} = \begin{bmatrix} 0 \\ E_f \\ 0 \end{bmatrix} - \begin{bmatrix} Z_0 & 0 & 0 \\ 0 & Z_1 & 0 \\ 0 & 0 & Z_2 \end{bmatrix} \begin{bmatrix} I_{a0} \\ I_{a1} \\ I_{a2} \end{bmatrix} \quad (1.29)$$

## 2.3 Analysis of Unbalanced Faults [18]

### 2.3.1 Single line-to ground faults

Single line to ground faults occurs when one of any three lines falls is on the ground.

Assume that the fault occurred on phase a with zero fault impedance as shown in figure 2.1.

Since the fault impedance is zero and load current is neglected, then at the fault point

$$V_a = 0 \qquad I_b = 0 \qquad I_c = 0 \tag{1.30}$$

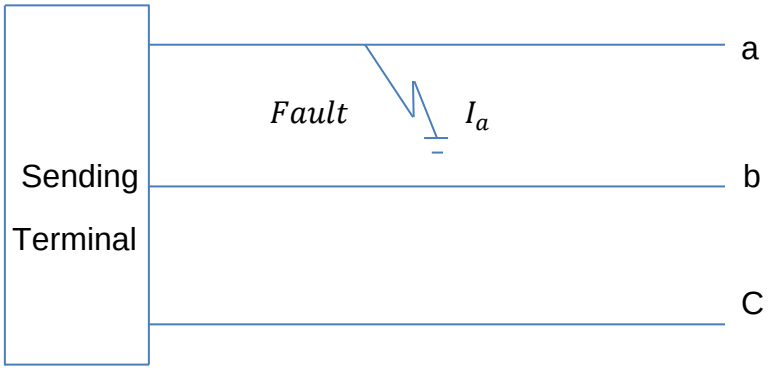


Figure 1.8 Single Line to ground fault on phase a

The fault condition can be converted to symmetrical component as

$$V_a = V_{a0} + V_{a1} + V_{a2} = 0 \tag{1.31}$$

$$\begin{bmatrix} I_{a0} \\ I_{a1} \\ I_{a2} \end{bmatrix} = \frac{1}{3}\begin{bmatrix} 1 & 1 & 1 \\ 1 & a & a^2 \\ 1 & a^2 & a \end{bmatrix}\begin{bmatrix} I_a \\ I_b = 0 \\ I_c = 0 \end{bmatrix} \tag{1.32}$$

We get

$$I_{a0} = I_{a1} = I_{a2} = \frac{I_a}{3} \tag{1.33}$$

With the fault current $I_f = I_a$ (1.34)

$$\begin{bmatrix} V_{a0} \\ V_{a1} \\ V_{a2} \end{bmatrix} = \begin{bmatrix} 0 \\ E_f \\ 0 \end{bmatrix} - \begin{bmatrix} Z_0 & 0 & 0 \\ 0 & Z_1 & 0 \\ 0 & 0 & Z_2 \end{bmatrix} \begin{bmatrix} I_{a0} = \frac{I_a}{3} \\ I_{a1} = \frac{I_a}{3} \\ I_{a2} = \frac{I_a}{3} \end{bmatrix} \tag{1.35}$$

$$V_{a0} = 0 - Z_0 \frac{I_a}{3} \tag{1.36}$$

$$V_{a1} = E_f - Z_1 \frac{I_a}{3} \tag{1.37}$$

$$V_{a2} = 0 - Z_2 \frac{I_a}{3} \tag{1.38}$$

Thus

$$V_{a0} + V_{a1} + V_{a2} = 0 = -Z_0 \frac{I_a}{3} + E_f - Z_1 \frac{I_a}{3} - Z_2 \frac{I_a}{3} \tag{1.39}$$

$$I_f = I_a = \frac{3E_f}{Z_1 + Z_2 + Z_0} \tag{1.40}$$

We can assume that the sequence component must be connected in series and short circuited because

$$V_{a0} + V_{a1} + V_{a2} = 0 \text{ and } I_{a0} = I_{a1} = I_{a2} \tag{1.41}$$

Assume that the fault occur on phase a through impedance $Z_f$ then to the ground.

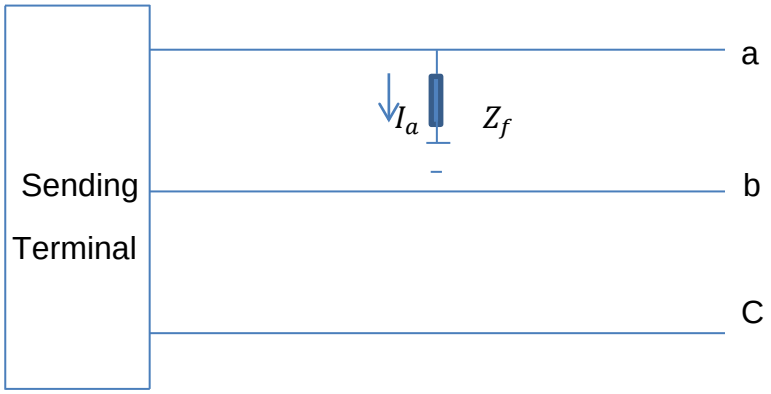


Figure 1.9 Single Line to ground fault on phase a with fault impedance

At the fault point we have

$$V_a = Z_f I_a \tag{1.42}$$

$$I_b = I_c = 0 \tag{1.43}$$

By using method of symmetrical component

$$V_{a0} + V_{a1} + V_{a2} = (I_{a0} + I_{a1} + I_{a2})Z_f \tag{1.44}$$

$$\begin{bmatrix} I_{a0} \\ I_{a1} \\ I_{a2} \end{bmatrix} = \frac{1}{3}\begin{bmatrix} 1 & 1 & 1 \\ 1 & a & a^2 \\ 1 & a^2 & a \end{bmatrix}\begin{bmatrix} I_a \\ I_b = 0 \\ I_c = 0 \end{bmatrix} \tag{1.45}$$

$$I_{a0} = I_{a1} = I_{a2} = \frac{I_a}{3} \tag{1.46}$$

$$V_{a0} + V_{a1} + V_{a2} = 3I_{a0}Z_f \tag{1.47}$$

Or

$$V_{a0} + V_{a1} + V_{a2} = I_{a0}3Z_f \tag{1.48}$$

Equating these equations

$$I_{fa0} = \frac{V_f}{Z_1+Z_2+Z_0+3Z_f} \tag{1.49}$$

Then $I_{a0} = I_{a1} = I_{a2}$ is the current injecting to the fault for the single line to ground

### 2.3.2 Line-to line faults

Line to line fault occurs when two lines come to contact to each other. Assume that the fault is on phase b and c with no fault impedance. The fault conditions for this type of fault are:

$$I_a = 0 \qquad I_b = -I_c \qquad V_b = V_c \tag{1.50}$$

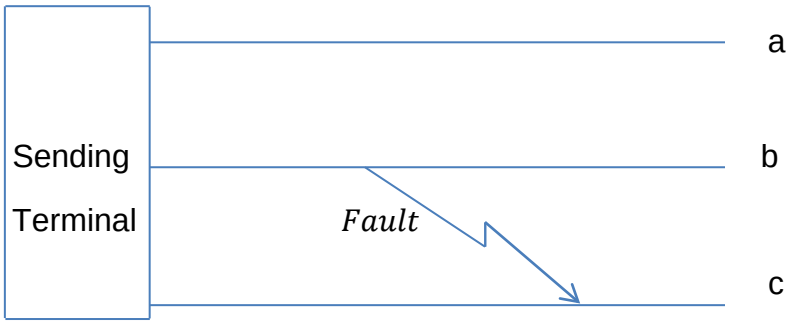


Figure 1.10 Line-to- Line fault

By using method of symmetrical component

$$\begin{bmatrix} I_{a0} \\ I_{a1} \\ I_{a2} \end{bmatrix} = \frac{1}{3}\begin{bmatrix} 1 & 1 & 1 \\ 1 & a & a^2 \\ 1 & a^2 & a \end{bmatrix}\begin{bmatrix} I_a = 0 \\ I_b \\ I_c = -I_b \end{bmatrix} \quad (1.51)$$

Then

$$I_{a0} = 0 \quad (1.52)$$

$$I_{a1} = \frac{1}{3}(a - a^2)I_b \quad (1.53)$$

$$I_{a2} = \frac{1}{3}(a^2 - a)I_b \quad (1.54)$$

We can assume that

$$I_{a0} = 0 \quad (1.55)$$

$$I_{a1} = \frac{1}{3}(a - a^2)I_b \quad (1.56)$$

$$I_{a2} = \frac{1}{3}(a^2 - a)I_b \quad (1.57)$$

We can assume that

$$I_{a1} = -I_{a2} \quad (1.58)$$

Or

$$I_{a1} + I_{a2} = 0 \quad (1.59)$$

The symmetrical component when $V_b = V_c$

$$\begin{bmatrix} V_{a0} \\ V_{a1} \\ V_{a2} \end{bmatrix} = \frac{1}{3}\begin{bmatrix} 1 & 1 & 1 \\ 1 & a & a^2 \\ 1 & a^2 & a \end{bmatrix}\begin{bmatrix} V_a \\ V_b \\ V_c = V_b \end{bmatrix} \quad (1.60)$$

We get

$$V_{a1} = V_{a2} \quad (1.61)$$

Then the boundary conditions are

$$I_{a0} = 0,\ I_{a1} + I_{a2} = 0 \text{ and } V_{a1} = V_{a2} \quad (1.62)$$

Assume that the fault is on phase b and c with fault impedance. If $Z_f$ is in the path between b and c the fault conditions for this type of fault are:

$$I_a = 0 \qquad I_b = -I_{fc} \qquad V_b - V_c = I_b Z_f \quad (1.63)$$

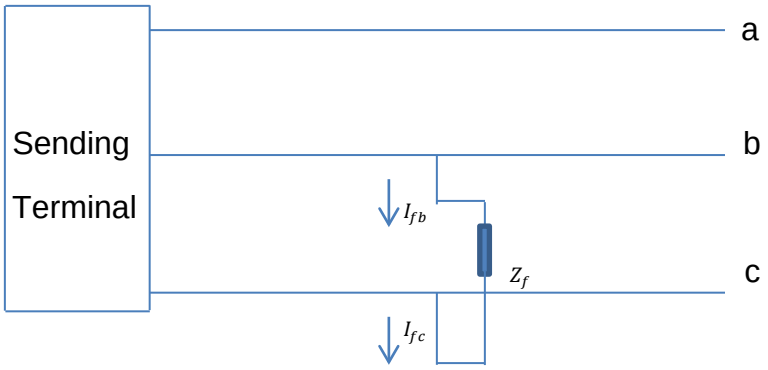


Figure 1.11 Line-to- Line fault with fault impedance

By using method of symmetrical component

$$\begin{bmatrix} I_{fa0} \\ I_{fa1} \\ I_{fa2} \end{bmatrix} = \frac{1}{3}\begin{bmatrix} 1 & 1 & 1 \\ 1 & a & a^2 \\ 1 & a^2 & a \end{bmatrix}\begin{bmatrix} 0 \\ I_{fb} \\ -I_{fb} \end{bmatrix} \quad (1.64)$$

Then

$$I_{fa0} = 0 \quad (1.65)$$

$$I_{fa1} = \frac{1}{3}(a - a^2)I_{fb} \quad (1.66)$$

$$I_{fa2} = \frac{1}{3}(a^2 - a)I_{fb} \quad (1.67)$$

We can assume that

$$I_{fa1} = -I_{fa2} \tag{1.68}$$

### 2.3.3 Double Line-to ground faults

Double line to ground faults occur when any two lines of three lines comes in contact with the ground. Assume that the fault occurs on phase b and phase c through impedance $Z_f$ to ground. The fault conditions for this type of fault are

$$I_{fa} = 0 \qquad V_{fb} = V_{fc} = (I_{fb} + I_{fc})Z_f \tag{1.69}$$

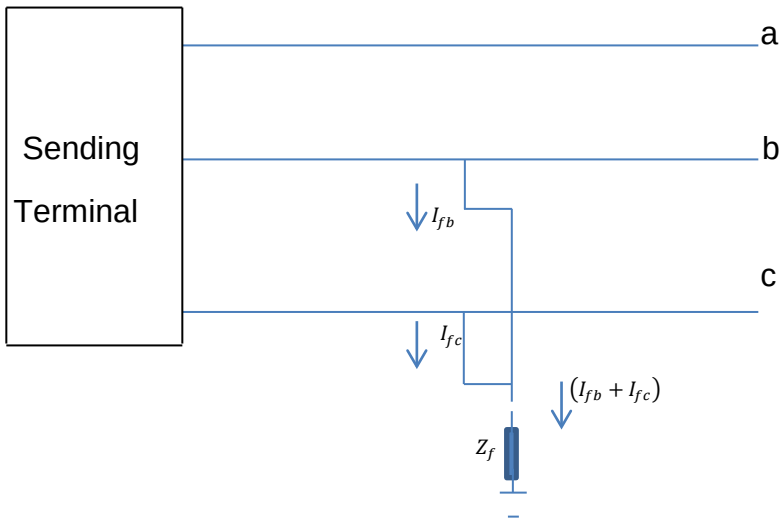


Figure1.12 Double Line-to ground fault

$$\begin{bmatrix} I_{fa0} \\ I_{fa1} \\ I_{fa2} \end{bmatrix} = \frac{1}{3}\begin{bmatrix} 1 & 1 & 1 \\ 1 & a & a^2 \\ 1 & a^2 & a \end{bmatrix}\begin{bmatrix} 0 \\ I_{fb} \\ I_{fc} \end{bmatrix} \tag{1.70}$$

$$I_{fa0} = \frac{1}{3}(I_{fb} + I_{fc}) \tag{1.71}$$

Since

$$V_b = V_c = (I_{fb} + I_{fc})Z_f \quad (1.72)$$

Then

$$V_b = V_c = 3Z_f I_{fa0} \quad (1.73)$$

Use the method of symmetrical component to find $V_{fb}$

$$\begin{bmatrix} V_{a0} \\ V_{a1} \\ V_{a2} \end{bmatrix} = \frac{1}{3}\begin{bmatrix} 1 & 1 & 1 \\ 1 & a & a^2 \\ 1 & a^2 & a \end{bmatrix}\begin{bmatrix} V_a \\ V_b \\ V_c \end{bmatrix} \quad (1.74)$$

$$V_{a1} = \frac{1}{3}(V_a + aV_b + a^2V_c) \quad (1.75)$$

$$V_{a2} = \frac{1}{3}(V_a + a^2V_b + aV_c) \quad (1.76)$$

Thus

$$V_{a1} = V_{a2} \quad (1.77)$$

$$V_{a0} = \frac{1}{3}(V_a + V_b + V_c) \quad (1.78)$$

Because $V_b = V_c$

$$3V_{a0} = V_a + 2V_b \quad (1.79)$$

$$= (V_{a0} + V_{a1} + V_{a2}) + 2(3Z_f I_{fa0}) \quad (1.80)$$

$$= \left(V_{a0} + 2V_{a1} + 2(3Z_f I_{fa0})\right) \quad (1.81)$$

$$2V_{a0} - 2(3Z_f I_{fa0}) = 2V_{a1} \quad (1.82)$$

We obtain

$$V_{a1} = V_{a0} - (3Z_f I_{fa0}) \quad (1.83)$$

The fault current can be obtained as

$$I_{fa0} = -I_{fa1}\left[\frac{Z_2}{Z_2+Z_0+3Z_f}\right] \quad (1.84)$$

$$I_{fa1} = \frac{V_f}{Z_1+\left[\frac{Z_2(Z_0+3Z_f)}{Z_2+Z_0+3Z_f}\right]} \quad (1.85)$$

$$I_{fa2} = -I_{fa1}\left[\frac{Z_0+3Z_f}{Z_2+Z_0+3Z_f}\right] \quad (1.86)$$

# CHAPTER TWO

# REVIEW OF LITERATURES

## Review of Existing Fault Location Algorithm

Many proposals for improving fault distance estimation for parallel transmission lines have been developed and presented in the past.

In [1], the mutual coupling impedances between the parallel transmission lines are presented. Zero-sequence mutual impedances are about 50-55% of the zero-sequence self-impedances and will lead to significant error if the calculation of the fault location does not take it into account.

In [2], the authors propose a method for parallel transmission line fault location using one-end data. Data obtained from the fault lines and sound line are utilized to derive the sequence phase voltage and sequence phase current equations at the relay location to calculate the fault distance by eliminating the terms containing the sequence current from the other end. With the boundary condition, the fault distance estimation can be obtained. However, while this method is independent of fault resistance, load currents, source impedance, and remote in-feed, yet shunt capacitance is neglected which might lead to errors in the calculation of fault distance.

In [3], one terminal algorithm using local voltages and current near end of the faulted line has been employed. The zero-sequence current from the near end of the healthy line is used as the input signals. The authors use the compensation techniques to compensate for the errors that cause from the fault resistance.

In [4], an adaptive protective relaying scheme for parallel-line distance protection is proposed. A detailed algorithm is used to improve the distance protection performance for parallel lines affected by mutual coupling effect. The algorithm takes into account the zero-sequence current of the parallel circuit to compensate for the mutual effect. To improve performance, the algorithm solves the problem based on zero sequence on the parallel line, the line operating status, and the default zero-sequence compensation factor, respectively.

J. Izykowski, E. Rosolowski, and M. Mohan Saha [5] proposed a fault location algorithm for parallel transmission lines by using the voltage and current phasors at one end. The complete measurement of the three-phase voltages and three-phase currents from a faulted line and a healthy line are measured by the fault locator. The fault current is calculated without the zero sequence by setting the current to zero to exclude the zero sequence components. According to the availability of complete measurements at one end, the derived algorithm is a very simple first-order form because the fault location algorithm does not include any source impedance, then the algorithm is not influenced by the varying source impedances or fault resistance

In A. Wiszniewski [6], an algorithm for locating fault on transmission line has been proposed. The accuracy of the fault location is affected by the fault resistance since the fault current through the fault resistance shifts in phase with the current measured at the end of the line. The algorithm will compensate and accurately locate the fault.

The authors in [7] present an algorithm that deals with non-earth faults on one of the circuits of parallel transmission line. Three voltage equations from one end to a faulty line to the fault point were established based on symmetrical component. Then adding these three equations together to form the equation with fault current and fault resistance as unknowns. By applying Kirchhoff voltage law(KVL) the fault current can be expressed as a function of fault location. Then fault resistance and fault location can be obtained by solving those equations. This algorithm does not consider shunt capacitance which may cause errors for the long transmission lines.

The authors of [8] propose a technique for using the data from two terminals of the transmission line to estimate fault location. The lumped parameter line model is adopted and the shunt capacitance for long transmission line is compensated in an iterative calculation. This technique is independent from the fault type, fault resistance, load current, and source impedance. Synchronization of data is not required for this technique. Real-time communication is not needed for this analysis, only the off-line post-fault analysis.

A new digital relaying technique for parallel transmission lines is presented in [9]. This technique uses only one relay at each end of the two terminals. The technique provides a simple protection technique without requiring any complex mathematics while avoiding software and hardware complications.

The author in [10] proposes a novel digital distance-relaying technique for transmission line protection. Two relays instead of four are used for a parallel

transmission line. One is at the beginning and the other is at the end. Each relay receives three voltages and six current signals from the parallel line. This technique compares the measured impedance of the corresponding phase. It solves the complexities of the type of faults, high fault resistance, mutual effects, and current in-feed.

In [11], the protection of double-circuit line using wavelet transform is proposed. The authors propose using the powerful analyzing and decomposing features of wavelet transform to solve the problems in a double transmission line when protected by a distance relay. The technique uses three-line voltages and six-line current of the parallel transmission lines at each end. The algorithm is based on a comparison of the detailed coefficient of corresponding phases. The proposed method will eliminate problems such as high fault resistance, cross-country fault, mutual coupling effect, current in-feed, and fault near a remote bus.

A high-resistance fault on two terminal parallel transmission lines is presented in [12]. The paper discusses the problems faced by a conventional non-pilot distance relay when protecting two terminal parallel transmission lines. These problems include ground fault resistance, prefault system conditions, mutual effects of parallel lines, and shunt capacitance influences. The paper also presents a detailed analysis of impedance by the taking into account the relaying point, mutual effects of parallel lines, shunt capacitance influences, and the system external to the protected line.

The authors in [13] propose avoiding under-reaching in twin circuit lines without residual current input from the parallel line. The mutual coupling effect is

one problem for transmission line protection from single phase-to-earth faults on multiple circuit towers. The zero sequence of the lines gets mutual coupled causing an error in the impedance seen by the relay. This causes the distance protection relay at one end of the faulty line to overreach and the relay at the other end to under-reach, which may lead to false trip of the healthy line. The authors propose the characteristic expression for the effectiveness experienced by a double circuit with and without mutual coupling and develop a non-iterative microprocessor-based real-time algorithm for computing fault distance and zero-sequence compensation in the distance relay scheme.

Reference [14] presents a method to locate the faults location in parallel transmission lines without any measurements from the healthy line circuit. The paper discusses a new one-end fault location algorithm for parallel transmission lines. The method considers the flow of currents for the zero sequence and utilizes the relation between the sequence components of a total fault current relevant for single phase-to ground faults. This allows reflecting the mutual coupling effect under phase-to ground faults without using the zero sequence current from the healthy line circuit.

In [15] the transmission line fault location methods have been presented. Instead of using both voltage and current, the method utilizes only the voltage as an input and eliminates the use of current that caused errors because of the saturation of current transformer. The fault location algorithms used unsynchronized voltage measured during the fault. The algorithm also considers

shunt capacitance. The source impedances are assumed to be available at two terminals.

Authors [16] present the method for deriving an optimal estimation of the fault location that can detect and identify the bad measurement to minimize the measurement errors for improving the fault location estimation. The derivation is based on the distributed parameter line model and fully considers the effect of shunt capacitance.

Author [17] presents the derivation of the equivalent PI circuit for the zero-sequence networks of a double-circuit line based on distributed parameter model. The author applies the symmetrical component transformation that result in positive sequence, negative sequence, and zero sequence. The mutual coupling effect is taking into account for zero sequence analysis and the effects of shunt capacitance and a long line effect is considered.

More references can be found in [18]-[24] regarding the studied subject.

The algorithm based on lumped parameter model is presented in [25] to introduce the errors for long transmission lines. The algorithm needs only the magnitude of the current from different terminal that is the different current in different circuit measured at the same terminal. Because of this algorithm is develop in three terminal parallel transmission line, thus each terminal network should be converted to an equivalent three terminal network. The algorithm needs only the differences of the current, thus synchronization of the terminal is not required. This algorithm is independent of the fault resistance and any source impedances.

Reference [26] presents a method to locate the faults location in parallel transmission lines due to the mutual coupling effects between circuits of the lines by using the data from only one end of the line. The algorithm is based on modifying the impedance method using modal transformation that transform the coupled equations of the transmission lines into decoupled equations, then the elimination of the mutual effects resulting in an accurate estimation for the fault location.

# CHAPTER THREE

# PROPOSED NEW FAULT LOCATION ALGORITHM FOR PARALLEL TRANSMISSION LINES

Each of the research proposals cited above for determining the transmission line fault location has its own advantages and disadvantages, depending on the availability of the system measurement. In this research, I will explore new methods for extracting a more accurate estimation of fault location in long parallel transmission lines by using the equivalent PI circuit based on a distributed parameter line model. The new method, assuming the local voltage and current are available, will fully consider the mutual coupling impedance, the mutual coupling admittance and shunt capacitance for high precision in fault distance estimation. This research builds upon and extends the work of [2] by accurately considering the shunt capacitances of lines.

## 1. MODEL USED

The new method uses only the voltage and current from one end of parallel lines to calculate the fault distance [2]. This method is independent of the fault resistance, remote infeed, and source impedance. This method is using shunt capacitance based on distributed parameter line model and mutual coupling between lines instead of lump parameter to improve the fault distance estimation for parallel transmission lines.

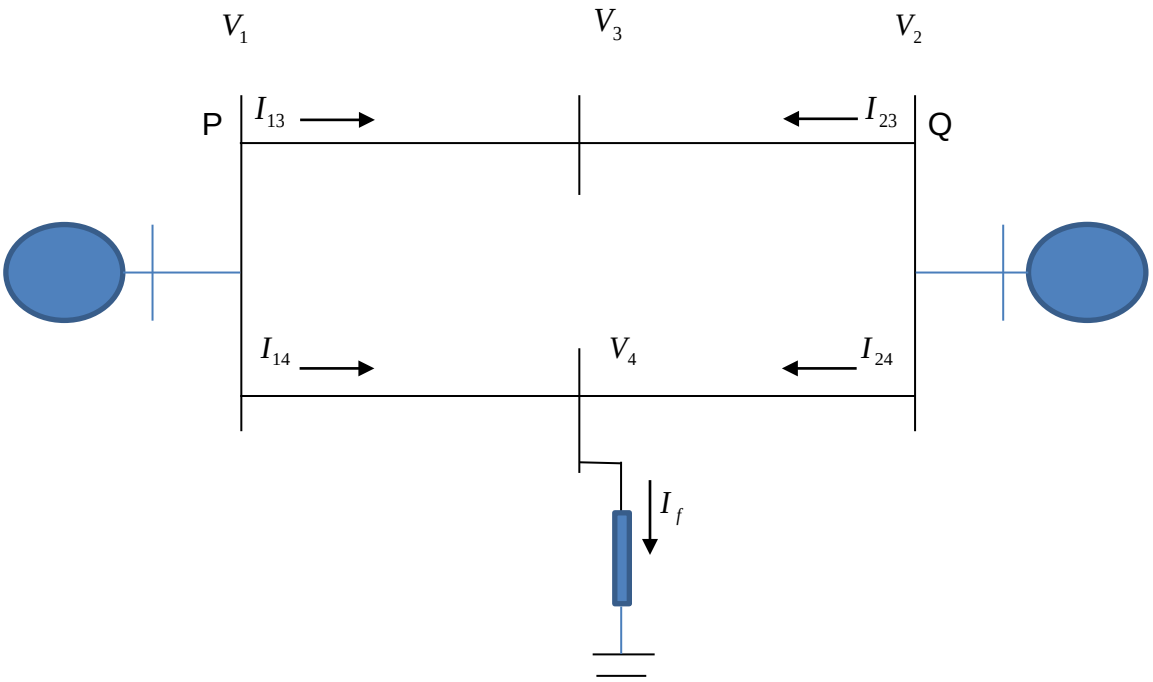


Figure3.1. System diagram used in the development of the new algorithm

To get the proposed algorithm to work, the power system model shown in fig. 1 is used to develop the method for improving fault distance estimation for parallel transmission lines using only voltage and current from only one end of the parallel transmission lines. This power system model consists of two generators, two parallel transmission lines and four buses: 1, 2, 3, and 4. We have assumed that one of the parallel lines is experiencing a fault at bus 4. After we have finished with the model, ATP-EMTP (Alternative Transient Program), special software for the simulation and analysis transient in power system, will be used for the simulation and analysis. The model will be designed to study transient state while fault occurs in the power system. ATP-EMTP has been utilized to generate fault cases under various fault conditions with different fault

locations, fault types and fault resistances. ATP-EMTP will give the outputs in voltage, current, power and energy versus times. All of the output files from ATP-EMTP simulation will be saved as an .atp file and then converted to a data file in .pl4 format for Matlab (Matrix laboratory) to use for analysis. In the other words, EMTP will give an output in time domain signals that is the simulation of the fault condition. Then we will use Matlab to convert time domain signals to frequency domain by using FFT to get phasors to use as input for the algorithm. In this research we assume that one of the parallel lines PQ that is 300 km long was selected to experience the fault at F. The fault is 100 km away from bus P with 10 ohms fault resistance. The system has the base voltage of 400 kV and frequency is 50 Hz. The transmission lines are fully distributed and the parameters of the transmission lines are obtained from the table below:

Table 3.1 Parameters per km of zero-sequence networks of a parallel line

| Parameter | Value |
|---|---|
| Series impedance(ohm/km) | 0.268+j1.0371 |
| Mutual impedance(ohm/km) | 0.23+j0.6308 |
| Shunt admittance(S/km) | j2.7018e-6 |
| Mutual admittance $\boldsymbol{y_m}$ (S/km) | j1.6242e-6 |

Table 3.2 Parameters per km of positive-sequence networks of a parallel lines

| Parameter | Value |
|---|---|
| Series impedance(ohm/km) | 0.061+j0.3513 |
| Shunt admittance(S/km) | j4.66e-6 |

Table 3.3.Source impedance at P and Q

| Parameter | Terminal P | Terminal Q |
|---|---|---|
| Positive-sequence source impedance(ohm) | 0.3190+j19.7544 | 0.4745+j28.6908 |
| Zero-sequence source impedance(ohm) | 0.2872+j8.4968 | 0.6829+j23.9267 |

Voltages and currents data in the system model at terminal P have been generated under various fault types and fault conditions. The data were utilized in the algorithm in [2] Y. Liao, S. Elangovan, “Digital Distance Relaying Algorithm for First-Zone Protection for Parallel Transmission Lines,” Proc.-Gener. Transm. Distrib. IEE, 1998, 145, (5), pp.531-536., to implement and evaluate the simulated data for fault distance and fault resistance The results shown above will be used to compare with the results of my proposed algorithm.

## 2. Proposed Equivalent PI Circuit Model for New Fault Location Algorithm for Parallel Transmission lines

The symmetrical component theory will be used to design the model. Shunt capacitance, mutual admittance, and mutual impedance have to be considered for zero sequence.

### 2.1 Positive Sequence Network

The positive sequence, the negative sequence, and zero sequence networks of the parallel transmission line are depicted in Figure 1, Figure 2, and Figure 3 respectively. The parallel circuits are assumed to have the same parameter. Buses are denoted by P and Q, while R is the fault location.

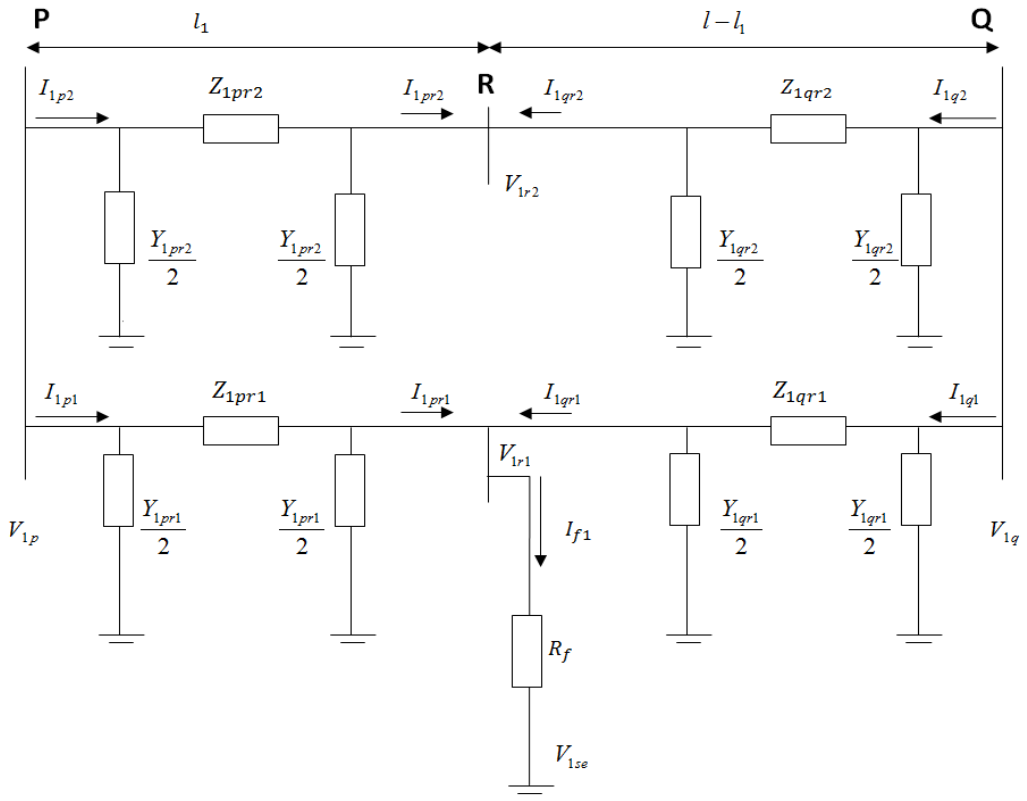


Figure 3.2. Equivalent PI circuit of positive sequence network of the system during the fault

In figure 14, the following notations are adopted:

$V_{1p}$ , $V_{1q}$ positive sequence voltage during the fault at P and Q

$V_{1r1}$, $V_{1r2}$ positive sequence voltage during the fault at R at line 1 and 2

$I_{1p1}$ , $I_{1q1}$ positive sequence current during the fault at P and Q at line 1

$I_{1pr1}$ , $I_{1qr1}$ positive sequence current during the fault at R at line 1

$I_{1p2}$ , $I_{1q2}$ Positive sequence current during the fault at P and Q at line 2

$I_{1pr2}$ , $I_{1qr2}$ positive sequence current during the fault at R at line 2

$Z_{1pr1}$ , $Z_{1qr1}$ equivalent series impedance of the line PR and QR at line 1

$Z_{1pr2}$ , $Z_{1qr2}$ equivalent series impedance of the line PR and QR at line 2

$Y_{1pr1}$ , $Y_{1qr1}$ equivalent shunt admittance of the line PR and QR at line 1

$Y_{1pr2}$ , $Y_{1qr2}$ equivalent shunt admittance of the line PR and QR at line 2

$I_{f1}$ positive sequence fault current at R

$l_1$ fault distance from P to R in mile or km

The equivalent line parameters are calculated based on the distributed parameter line model as [17]:

$$Z_{1c1} = \sqrt{z_{1s1}/y_{1s1}} \quad (3.1)$$

$$\gamma_{1s1} = \sqrt{z_{1s1}y_{1s1}} \quad (3.2)$$

$$Z_{1c2} = \sqrt{z_{1s2}/y_{1s2}} \quad (3.3)$$

$$\gamma_{1s2} = \sqrt{z_{1s2}y_{1s2}} \quad (3.4)$$

Where

$Z_{1c1}$ characteristic impedance of the line 1

$\gamma_{1s1}$ propagation constant of the line 1

$Z_{1c2}$ characteristic impedance of the line 2

$\gamma_{1s2}$ propagation constant of the line 2

$z_{1s1}$, $y_{1s1}$ positive sequence series impedance and shunt admittance of line 1 per mile or km, respectively.

$z_{1s2}$, $y_{1s2}$ positive sequence series impedance and shunt admittance of line 2 per mile or km, respectively.

$$Z_{1pr1} = Z_{1c1}\sinh(\gamma_{1s1}l_1) \quad (3.5)$$

$$Z_{1qr1} = Z_{1c1}\sinh[\gamma_{1s1}(l-l_1)] \quad (3.6)$$

$$Z_{1pr2} = Z_{1c2}\sinh(\gamma_{1s2}l_1) \quad (3.7)$$

$$Z_{1qr2} = Z_{1c2}\sinh[\gamma_{1s2}(l-l_1)] \quad (3.8)$$

$$Y_{1pr1} = \frac{2}{Z_{1c1}}\tanh\left(\frac{\gamma_{1s1}l_1}{2}\right) \quad (3.9)$$

$$Y_{1qr1} = \frac{2}{Z_{1c1}}\tanh\left[\frac{\gamma_{1s1}(l-l_1)}{2}\right] \quad (3.10)$$

$$Y_{1pr2} = \frac{2}{Z_{1c2}}\tanh\left(\frac{\gamma_{1s2}l_1}{2}\right) \quad (3.11)$$

$$Y_{1qr2} = \frac{2}{Z_{1c2}}\tanh\left[\frac{\gamma_{1s2}(l-l_1)}{2}\right] \quad (3.12)$$

## 2.2 Negative Sequence Network

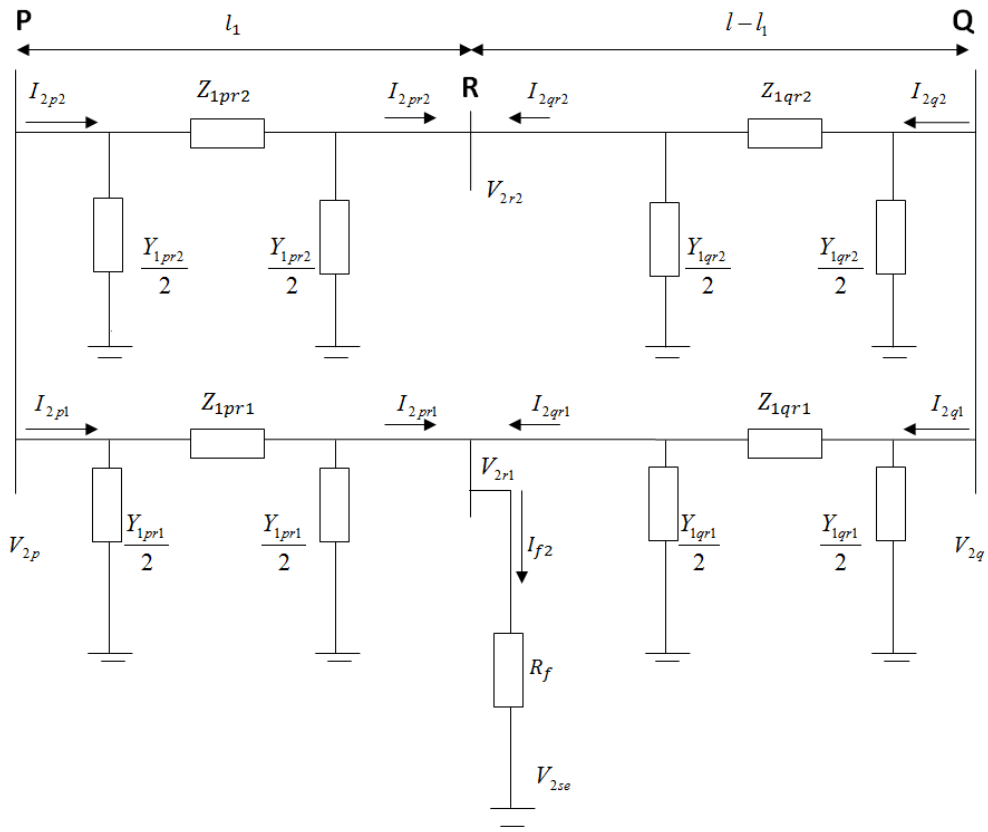


Figure 3.3.Equivalent PI circuit of negative sequence network of the system during the fault

In figure 15, the following notations are adopted:

$V_{2p}$ , $V_{2q}$ Negative sequence voltage during the fault at P and Q

$V_{2r1}$, $V_{2r2}$ Negative sequence voltage during the fault at R at line 1 and 2 respectively

$I_{2p1}$ , $I_{2q1}$ Negative sequence current during the fault at P and Q at line 1

$I_{2pr1}$ , $I_{2qr1}$ Negative sequence current during the fault at R at line 1

$I_{2p2}$ , $I_{2q2}$ Negative sequence current during the fault at P and Q at line 2

$I_{2pr2}$ , $I_{2qr2}$ Negative sequence current during the fault at R at line 2

$Z_{1pr1}$ , $Z_{1qr1}$ equivalent series impedance of the line PR and QR at line 1

$Z_{1pr2}$ , $Z_{1qr2}$ equivalent series impedance of the line PR and QR at line 2

$Y_{1pr1}$ , $Y_{1qr1}$ Equivalent shunt admittance of the line PR and QR at line 1

$Y_{1pr2}$ , $Y_{1qr2}$ Equivalent shunt admittance of the line PR and QR at line 2

$I_{f2}$ Negative sequence fault current at R

$l_1$ Fault distance from P to R in mile or km

The equivalent line parameters are calculated based on the distributed parameter line model as[17]:

$$\boldsymbol{Z_{1c1}} = \sqrt{\boldsymbol{z_{1s1}/y_{1s1}}} \quad (3.13)$$

$$\boldsymbol{\gamma_{1s1}} = \sqrt{\boldsymbol{z_{1s1}y_{1s1}}} \quad (3.14)$$

$$\boldsymbol{Z_{1c2}} = \sqrt{\boldsymbol{z_{1s2}/y_{1s2}}} \quad (3.15)$$

$$\boldsymbol{\gamma_{1s2}} = \sqrt{\boldsymbol{z_{1s2}y_{1s2}}} \quad (3.16)$$

Where

$Z_{1c1}$ characteristic impedance of the line 1

$\gamma_{1s1}$ propagation constant of the line 1

$Z_{1c2}$ characteristic impedance of the line 2

$\gamma_{1s2}$ propagation constant of the line 2

$z_{1s1}$, $y_{1s1}$ positive sequence series impedance and shunt admittance of line 1 per mile or km, respectively.

$z_{1s2}$, $y_{1s2}$ positive sequence series impedance and shunt admittance of line 2 per mile or km, respectively.

$$\boldsymbol{Z_{1pr1} = Z_{1c1}\sinh(\gamma_{1s1} l_1)} \quad (3.17)$$

$$\boldsymbol{Z_{1qr1} = Z_{1c1}\sinh[\gamma_{1s1}(l - l_1)]} \quad (3.18)$$

$$\boldsymbol{Z_{1pr2} = Z_{1c2}\sinh(\gamma_{1s2} l_1)} \quad (3.19)$$

$$\boldsymbol{Z_{1qr2} = Z_{1c2}\sinh[\gamma_{1s2}(l - l_1)]} \quad (3.20)$$

$$\boldsymbol{Y_{1pr1} = \frac{2}{Z_{1c1}}\tanh\left(\frac{\gamma_{1s1} l_1}{2}\right)} \quad (3.21)$$

$$\boldsymbol{Y_{1qr1} = \frac{2}{Z_{1c1}}\tanh\left[\frac{\gamma_{1s1}(l - l_1)}{2}\right]} \quad (3.22)$$

$$\boldsymbol{Y_{1pr2} = \frac{2}{Z_{1c2}}\tanh\left(\frac{\gamma_{1s2} l_1}{2}\right)} \quad (3.23)$$

$$\boldsymbol{Y_{1qr2} = \frac{2}{Z_{1c2}}\tanh\left[\frac{\gamma_{1s2}(l - l_1)}{2}\right]} \quad (3.24)$$

## 2.3 Zero Sequence Network

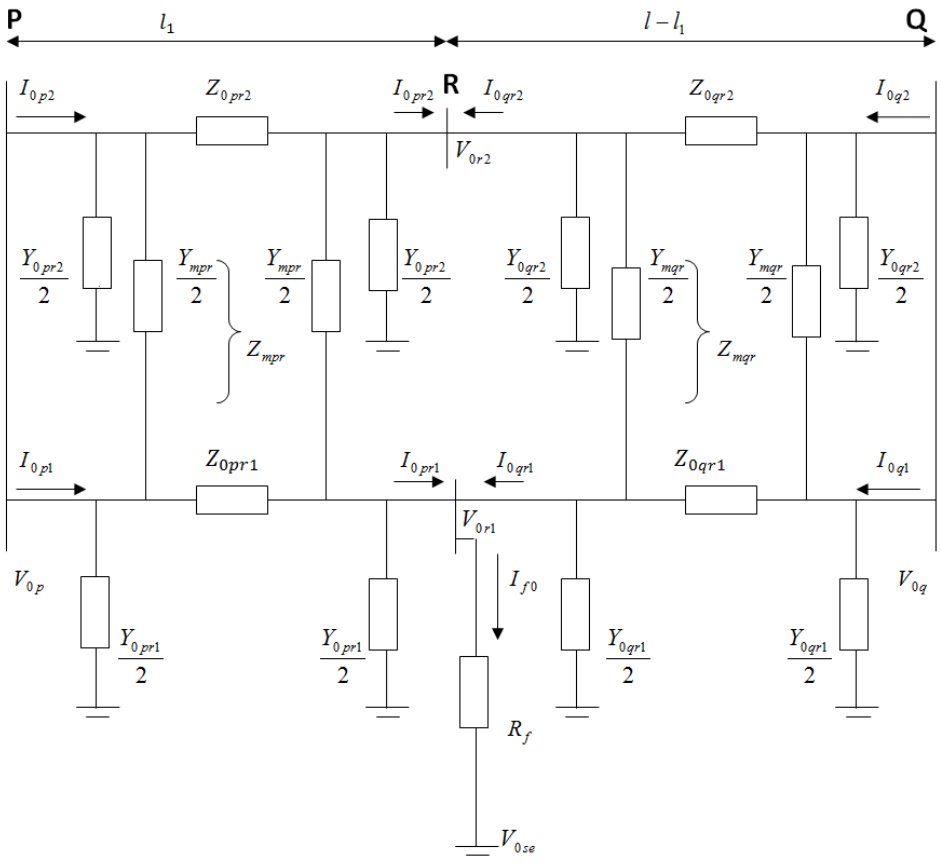


Figure 3.4.Equivalent PI circuit of mutually coupled zero-sequence network of the system during the fault

In figure 16, the following notations are adopted:

$V_{0p}$ , $V_{0q}$ zero sequence voltage during the fault at P and Q

$V_{0r1}$ , $V_{0r2}$ zero sequence voltage during the fault at R at line 1 and 2

$\boldsymbol{I_{0p1}}$ , $\boldsymbol{I_{0q1}}$ zero sequence current during the fault at P and Q at line 1

$\boldsymbol{I_{0pr1}}$ , $\boldsymbol{I_{0qr1}}$ zero sequence current during the fault at R at line 1

$\boldsymbol{I_{0p2}}$ , $\boldsymbol{I_{0q2}}$ zero sequence current during the fault at P and Q at line 2

$\boldsymbol{I_{0pr2}}$ , $\boldsymbol{I_{0qr2}}$ zero sequence current during the fault at R at line 2

$\boldsymbol{Z_{pr1}}$ , $\boldsymbol{Z_{0qr1}}$ equivalent series impedance of the line PR and QR at line 1

$\boldsymbol{Z_{pr2}}$ , $\boldsymbol{Z_{0qr2}}$ equivalent series impedance of the line PR and QR at line 2

$\boldsymbol{Y_{0pr1}}$ , $\boldsymbol{Y_{0qr1}}$ equivalent shunt admittance of the line PR and QR at line 1

$\boldsymbol{Y_{0pr2}}$ , $\boldsymbol{Y_{0qr2}}$ equivalent shunt admittance of the line PR and QR at line 2

$Y$ , $Y_m$ total equivalent self and mutual shunt admittance

$Z$ , $Z_m$ total equivalent self and mutual series impedance

$y$ shelf shunt admittance of the line per unit length

$y_m$ mutual shunt admittance between line per unit length

$z$ self-series impedance between lines per unit length

$z_m$ mutual series impedance between lines per unit length

$I_{f0}$ zero sequence fault current at R

$l_1$ fault distance from P to R in mile or km

In the mode domain, define

$$\boldsymbol{Z_{cm1}} = \sqrt{(\boldsymbol{z} - \boldsymbol{z_m})/(\boldsymbol{y} + \boldsymbol{2y_m})} \quad (3.25)$$

$$\boldsymbol{Z_{cm2}} = \sqrt{(\boldsymbol{z} - \boldsymbol{z_m})/\boldsymbol{y}} \quad (3.26)$$

$$\boldsymbol{\gamma_{m1}} = \sqrt{(\boldsymbol{z} - \boldsymbol{z_m})(\boldsymbol{y} + \boldsymbol{2y_m})} \quad (3.27)$$

$$\boldsymbol{\gamma_{m2}} = \sqrt{(\boldsymbol{z} + \boldsymbol{z_m})\boldsymbol{y}} \quad (3.28)$$

$$Z_{0pr1} = \frac{1}{2}[Z_{cm2}\sinh(\gamma_{m2}l_1) + Z_{cm1}\sinh(\gamma_{m1}l_1)] \quad (3.29)$$

$$Z_{0pr2} = \frac{1}{2}[Z_{cm2}\sinh(\gamma_{m2}l_1) + Z_{cm1}\sinh(\gamma_{m1}l_1)] \quad (3.30)$$

$$Z_{0qr1} = \frac{1}{2}\left[Z_{cm2}\sinh\left(\gamma_{m2}(l-l_1)\right) + Z_{cm1}\sinh\left(\gamma_{m1}(l-l_1)\right)\right] \quad (3.31)$$

$$Z_{0qr2} = \frac{1}{2}\left[Z_{cm2}\sinh\left(\gamma_{m2}(l-l_1)\right) + Z_{cm1}\sinh\left(\gamma_{m1}(l-l_1)\right)\right] \quad (3.32)$$

$$Z_{mpr} = \frac{1}{2}[Z_{cm2}\sinh(\gamma_{m2}l_1) - Z_{cm1}\sinh(\gamma_{m1}l_1)] \quad (3.33)$$

$$Z_{mqr} = \frac{1}{2}\left[Z_{cm2}\sinh\left(\gamma_{m2}(l-l_1)\right) - Z_{cm1}\sinh\left(\gamma_{m1}(l-l_1)\right)\right] \quad (3.34)$$

$$Y_{0pr1} = \frac{2\tanh(\gamma_{m2}l_1/2)}{Z_{cm2}} \quad (3.35)$$

$$Y_{0pr2} = \frac{2\tanh(\gamma_{m2}l_1/2)}{Z_{cm2}} \quad (3.36)$$

$$Y_{0qr1} = \frac{2\tanh(\gamma_{m2}(l-l_1)/2)}{Z_{cm2}} \quad (3.37)$$

$$Y_{0qr2} = \frac{2\tanh(\gamma_{m2}(l-l_1)/2)}{Z_{cm2}} \quad (3.38)$$

$$Y_{mpr} = \frac{\tanh(\gamma_{m1}l_1/2)}{Z_{cm1}} - \frac{\tanh(\gamma_{m2}l_1/2)}{Z_{cm2}} \quad (3.39)$$

$$Y_{mqr} = \frac{\tanh(\gamma_{m1}(l-l_1)/2)}{Z_{cm1}} - \frac{\tanh(\gamma_{m2}(l-l_1)/2)}{Z_{cm2}} \quad (3.40)$$

## 2.4 Proposed Distributed Parameter Line Model Based Algorithm

The distributed parameter line model will be adopted for the long transmission lines. Based on the sequence networks, the following equations are obtained:

Positive Sequence:

$$V_{1p} = \left( V_{1r1} \frac{Y_{1pr1}}{2} + I_{1pr1} \right) Z_{1pr1} + V_{1r1} \tag{3.41}$$

$$I_{1p1} = V_{1p} \frac{Y_{1pr1}}{2} + V_{1r1} \frac{Y_{1pr1}}{2} + I_{1pr1} \tag{3.42}$$

$$V_{1p} = \left( V_{1r2} \frac{Y_{1pr2}}{2} + I_{1pr2} \right) Z_{1pr2} + V_{1r2} \tag{3.43}$$

$$I_{1p2} = V_{1p} \frac{Y_{1pr2}}{2} + V_{1r2} \frac{Y_{1pr2}}{2} + I_{1pr2} \tag{3.44}$$

$$V_{1q} = \left( V_{1r1} \frac{Y_{1qr1}}{2} + I_{1qr1} \right) Z_{1pr2} + V_{1r1} \tag{3.45}$$

$$I_{1q1} = V_{1q} \frac{Y_{1qr1}}{2} + V_{1r1} \frac{Y_{1qr1}}{2} + I_{1qr1} \tag{3.46}$$

$$V_{1q} = \left( V_{1r2} \frac{Y_{1qr2}}{2} + I_{1qr2} \right) Z_{1qr2} + V_{1r2} \tag{3.47}$$

$$I_{1q2} = V_{1q} \frac{Y_{1qr2}}{2} + V_{1r2} \frac{Y_{1qr2}}{2} + I_{1qr2} \tag{3.48}$$

$$V_{1r1} = \left( I_{1pr1} + I_{1qr1} \right) R_f + V_{1se} \tag{3.49}$$

$$V_{1r2} = V_{1p} - \left( I_{1p2} - V_{1p} \frac{Y_{1pr2}}{2} \right) Z_{1pr2} \tag{3.50}$$

Negative Sequence:

$$V_{2p} = \left( V_{2r1} \frac{Y_{1pr1}}{2} + I_{2pr1} \right) Z_{1pr1} + V_{2r1} \tag{3.51}$$

$$I_{2p1} = V_{2p} \frac{Y_{1pr1}}{2} + V_{2r1} \frac{Y_{1pr1}}{2} + I_{2pr1} \tag{3.52}$$

$$V_{2p} = \left( V_{2r2} \frac{Y_{1pr2}}{2} + I_{2pr2} \right) Z_{1pr2} + V_{2r2} \tag{3.53}$$

$$I_{2p2} = V_{2p} \frac{Y_{1pr2}}{2} + V_{2r2} \frac{Y_{1pr2}}{2} + I_{2pr2} \tag{3.54}$$

$$V_{2q} = \left( V_{2r1} \frac{Y_{1qr1}}{2} + I_{2qr1} \right) Z_{1pr1} + V_{2r1} \tag{3.55}$$

$$I_{2q1} = V_{2q} \frac{Y_{1qr1}}{2} + V_{2r1} \frac{Y_{1qr1}}{2} + I_{2qr1} \tag{3.56}$$

$$V_{2q} = \left( V_{2r2} \frac{Y_{1qr2}}{2} + I_{2qr2} \right) Z_{1qr2} + V_{2r2} \tag{3.57}$$

$$I_{2q2} = V_{2q} \frac{Y_{1qr2}}{2} + V_{2r2} \frac{Y_{1qr2}}{2} + I_{2qr2} \tag{3.58}$$

$$V_{2r1} = \left( I_{2pr1} + I_{2qr1} \right) R_f + V_{2se} \tag{3.59}$$

$$V_{2r2} = V_{2p} - \left( I_{2p2} - V_{2p} \frac{Y_{1pr2}}{2} \right) Z_{1pr2} \tag{3.60}$$

Zero Sequence:

We have:

$$\frac{d}{dx}\begin{bmatrix} V_1 \\ V_2 \end{bmatrix} = \begin{bmatrix} Z_1 & Z_m \\ Z_m & Z_2 \end{bmatrix}\begin{bmatrix} I_1 \\ I_2 \end{bmatrix} \tag{3.61}$$

$$\frac{d}{dx}\begin{bmatrix} I_1 \\ I_2 \end{bmatrix} = \begin{bmatrix} y_1 + y_m & -y_m \\ -y_m & y_2 + y_m \end{bmatrix}\begin{bmatrix} V_1 \\ V_2 \end{bmatrix} \tag{3.62}$$

Where,

$z_1, z_2$ self series impedance per unit length of line 1 and line 2 respectively

$y_1, y_2$ self shunt admittance per unit length of line 1 and line 2 respectively

Transformation matrices and $T_i$

$$T_v^{-1}\begin{bmatrix} z_1 & z_m \\ z_m & z_2 \end{bmatrix} T_i = \begin{bmatrix} z_{m1} & 0 \\ 0 & z_{m2} \end{bmatrix} \tag{3.63}$$

$$T_i^{-1}\begin{bmatrix} y_1 + y_m & -y_m \\ -y_m & y_2 + y_m \end{bmatrix} T_v = \begin{bmatrix} y_{m1} & 0 \\ 0 & y_{m2} \end{bmatrix} \tag{3.64}$$

Then we can define

$$T_v = \begin{bmatrix} a_{11} & a_{12} \\ a_{21} & a_{22} \end{bmatrix} \tag{3.65}$$

$$T_v^{-1} = \begin{bmatrix} A_{11} & A_{12} \\ A_{21} & A_{22} \end{bmatrix} \tag{3.66}$$

The following equations are derived:

$$V_{0p} = \left( I_{0p1} - V_{0p}\frac{Y_{0pr1}}{2} - V_{0p}\frac{Y_{mpr}}{2} + V_{op}\frac{Y_{mpr}}{2} \right) Z_{0pr1} + \left( I_{0p2} - V_{0p}\frac{Y_{0pr2}}{2} - V_{0p}\frac{Y_{mpr}}{2} + V_{0p}\frac{Y_{mpr}}{2} \right) Z_{mpr} + V_{0r1} \quad (3.67)$$

$$I_{0p1} = V_{0p}\frac{Y_{0pr1}}{2} + V_{0p}\frac{Y_{mpr}}{2} - V_{0p}\frac{Y_{mpr}}{2} \quad (3.68)$$

$$V_{0p} = \left( I_{0p2} - V_{0p}\frac{Y_{0pr2}}{2} - V_{0p}\frac{Y_{mpr}}{2} + V_{op}\frac{Y_{mpr}}{2} \right) Z_{0pr2} + \left( I_{0p1} - V_{0p}\frac{Y_{0pr1}}{2} - V_{0p}\frac{Y_{mpr}}{2} + V_{0p}\frac{Y_{mpr}}{2} \right) Z_{mpr} + V_{0r2} \quad (3.69)$$

$$I_{0p2} = V_{0p}\frac{Y_{0pr2}}{2} + V_{0p}\frac{Y_{mpr}}{2} - V_{0p}\frac{Y_{mpr}}{2} \quad (3.70)$$

$$V_{0q} = \left( I_{0q1} - V_{0q}\frac{Y_{0qr1}}{2} - V_{0q}\frac{Y_{mqr}}{2} + V_{oq}\frac{Y_{mqr}}{2} \right) Z_{0qr1} + \left( I_{0q2} - V_{0q}\frac{Y_{0qr2}}{2} - V_{0q}\frac{Y_{mqr}}{2} + V_{0q}\frac{Y_{mqr}}{2} \right) Z_{mqr} + V_{0r1} \quad (3.71)$$

$$I_{0q1} = V_{0q}\frac{Y_{0qr1}}{2} + V_{0q}\frac{Y_{mqr}}{2} - V_{0q}\frac{Y_{mqr}}{2} \quad (3.72)$$

$$V_{0q} = \left( I_{0q2} - V_{0q}\frac{Y_{0qr2}}{2} - V_{0q}\frac{Y_{mqr}}{2} + V_{oq}\frac{Y_{mqr}}{2} \right) Z_{0qr2} + \left( I_{0q1} - V_{0q}\frac{Y_{0qr1}}{2} - V_{0q}\frac{Y_{mqr}}{2} + V_{0q}\frac{Y_{mqr}}{2} \right) Z_{mqr} + V_{0r2} \quad (3.73)$$

$$I_{0q2} = V_{0q}\frac{Y_{0qr2}}{2} + V_{0q}\frac{Y_{mqr}}{2} - V_{0q}\frac{Y_{mqr}}{2} \quad (3.74)$$

$$V_{0r1} = \left( I_{0pr1} + I_{0qr1} \right) R_f + V_{0se} \quad (3.75)$$

These equations form the basis for developing the fault location algorithm for different types of faults as described in the next section.

## 2.5 Proposed New Method to Estimate Fault Distance and Fault Resistance

The new method will approach the problem by deriving all equations from positive sequence, negative sequence, and zero sequence network by using KVL and KCL. Then, this research will employ function in Matlab program called Fsolve for iterative calculation.

An a-g type of fault will be considered first, and then the other types of fault will be tackled later. The boundary condition for an a-g fault is

$$V_{0se} + V_{1se} + V_{2se} = 0 \tag{3.76}$$

The transformation below will be adopted:

$$\begin{bmatrix} V_a \\ V_b \\ V_c \end{bmatrix} = \begin{bmatrix} 1 & 1 & 1 \\ 1 & a^2 & a \\ 1 & a & a^2 \end{bmatrix} \begin{bmatrix} V_0 \\ V_1 \\ V_2 \end{bmatrix} \tag{3.77}$$

Where

$$a = 1\angle 120^o = \frac{-1}{2} + j\frac{\sqrt{3}}{2} \tag{3.78}$$

The zero, positive, and negative sequence of each phase can be derived as follow:

$$\begin{bmatrix} V_0 \\ V_1 \\ V_2 \end{bmatrix} = \frac{1}{3}\begin{bmatrix} 1 & 1 & 1 \\ 1 & a & a^2 \\ 1 & a^2 & a \end{bmatrix} \begin{bmatrix} V_a \\ V_b \\ V_c \end{bmatrix} \tag{3.79}$$

And the same for current:

$$\begin{bmatrix} I_0 \\ I_1 \\ I_2 \end{bmatrix} = \frac{1}{3}\begin{bmatrix} 1 & 1 & 1 \\ 1 & a & a^2 \\ 1 & a^2 & a \end{bmatrix} \begin{bmatrix} I_a \\ I_b \\ I_c \end{bmatrix} \tag{3.80}$$

### 2.5.1 Proposed Algorithm

This research approaches the problem by deriving all equations from positive sequence, negative sequence, and zero sequence network by using KVL and KCL. Then, the fault location is obtained by solving these equations. The Newton-Raphson approach can be used to solve the unknowns as follows.

Define the following function vector:

$$\boldsymbol{f_i = 0,\ i = 1, \dots 2} \tag{3.81}$$

$$\boldsymbol{f_{1=real(f)}} \tag{3.82}$$

$$\boldsymbol{f_{2=imaj(f)}} \tag{3.83}$$

$$\text{f(x)} = [\boldsymbol{f_1(x), f_2(x)}]^{\boldsymbol{T}} \tag{3.84}$$

The Jacobian matrix J(x) is calculated as:

$$\text{Jij (x)} = \frac{\boldsymbol{\partial f_i(x)}}{\boldsymbol{\partial x_j}}\ , \boldsymbol{i = 1, \dots, 2, j = 1, \dots, 2} \tag{3.85}$$

Where

Jij (x) the element in $\boldsymbol{i^{th}}$ row and $\boldsymbol{j^{th}}$ column of J(x)

The unknown can be obtained following an iterative procedure. In the $\boldsymbol{k^{th}}$ iteration, the unknowns are updated using equation

$$\boldsymbol{x_{k+1} = x_k - \Delta x} \tag{3.86}$$

$$\Delta x = [J(x_k)]^{-1} f(x_k) \tag{3.87}$$

Where

$x_k\ , x_{k+1}$ the value of x before and after $k^{th}$ iteration, respectively;

$\Delta x$ update for $x\ and\ k^{th}$ iteration;

$k$ iteration number starting from 1

The iteration can be terminated when the update $\Delta x$ is smaller than the specified tolerance.

The unknown variables can be obtained by solving these equations and then boundary condition for each type of faults will be employed.

Positive Sequence:

$$V_{1r1\_left} = V_{1p} - Z_{1pr1}\left(I_{1p1} - V_{1p}\frac{Y_{1pr1}}{2}\right) \tag{3.88}$$

$$I_{1pr1} = I_{1p1} - V_{1p}\frac{Y_{1pr1}}{2} - V_{1r1\_left}\frac{Y_{1pr1}}{2} \tag{3.89}$$

$$V_{1r2} = V_{1p} - Z_{1pr2}\left(I_{1p2} - V_{1p}\frac{Y_{1pr2}}{2}\right) \tag{3.90}$$

$$I_{1pr2} = I_{1p2} - V_{1p}\frac{Y_{1pr2}}{2} - V_{1r2}\frac{Y_{1pr2}}{2} \tag{3.91}$$

$$V_{1q} = V_{1r2} - Z_{1qr2}\left(I_{1pr2} - V_{1r2}\frac{Y_{1qr2}}{2}\right) \tag{3.92}$$

$$V_{1r1\_right} = V_{1q} - Z_{1qr1}\left(I_{1q1} - V_{1q}\frac{Y_{1qr1}}{2}\right) \tag{3.93}$$

$$I_{1q1} = \left(\frac{V_{1q} - V_{1r1\_left}}{Z_{1qr1}}\right) + V_{1q}\frac{Y_{1qr1}}{2} \tag{3.94}$$

$$I_{1qr1} = I_{1q1} - V_{1q}\frac{Y_{1qr1}}{2} - V_{1r1\_left}\frac{Y_{1qr1}}{2} \tag{3.95}$$

$$I_{f1} = I_{1pr1} + I_{1qr1} \tag{3.96}$$

$$V_{1se} = V_{1r1\_left} - R_f I_{f1} \tag{3.97}$$

Negative Sequence:

$$V_{2r1\_left} = V_{2p} - Z_{1pr1}\left(I_{2p1} - V_{2p}\frac{Y_{1pr1}}{2}\right) \quad (3.98)$$

$$I_{2pr1} = I_{2p1} - V_{2p}\frac{Y_{1pr1}}{2} - V_{2r1\_left}\frac{Y_{1pr1}}{2} \quad (3.99)$$

$$V_{2r2} = V_{2p} - Z_{1pr2}\left(I_{2p2} - V_{2p}\frac{Y_{1pr2}}{2}\right) \quad (3.100)$$

$$I_{2pr2} = I_{2p2} - V_{2p}\frac{Y_{1pr2}}{2} - V_{2r2}\frac{Y_{1pr2}}{2} \quad (3.101)$$

$$V_{2q} = V_{2r2} - Z_{1qr2}\left(I_{2pr2} - V_{2r2}\frac{Y_{1qr2}}{2}\right) \quad (3.102)$$

$$V_{2r1\_right} = V_{2q} - Z_{1qr1}\left(I_{2q1} - V_{2q}\frac{Y_{1qr1}}{2}\right) \quad (3.103)$$

$$I_{2q1} = \left(\frac{V_{2q} - V_{2r1\_left}}{Z_{1qr1}}\right) + V_{2q}\frac{Y_{1qr1}}{2} \quad (3.104)$$

$$I_{2qr1} = I_{2q1} - V_{2q}\frac{Y_{1qr1}}{2} - V_{2r1\_left}\frac{Y_{1qr1}}{2} \quad (3.105)$$

$$I_{f2} = I_{2pr1} + I_{2qr1} \quad (3.106)$$

$$V_{2se} = V_{2r1\_left} - R_f I_{f2} \quad (3.107)$$

Zero Sequence:

$$V_{0r2} = V_{0p} - Z_{0pr2}\left(I_{0p2} - V_{0p}\frac{Y_{0pr2}}{2}\right) - Z_{mpr}\left(I_{0p1} - V_{0p}\frac{Y_{0pr2}}{2}\right) \tag{3.108}$$

$$V_{0r1\_left} = V_{0p} - Z_{0pr1}\left(I_{0p1} - V_{0p}\frac{Y_{0pr1}}{2}\right) - Z_{mpr}\left(I_{0p2} - V_{0p}\frac{Y_{0pr2}}{2}\right) \tag{3.109}$$

$$I_{0pr1} = I_{0p1} - V_{0p}\frac{Y_{0pr1}}{2} - V_{0r1\_left}\frac{Y_{0pr1}}{2} - \left(V_{0r1\_left} - V_{0r2}\right)\frac{Y_{mpr}}{2} \tag{3.110}$$

$$I_{0pr2} = I_{0p2} - V_{0p}\frac{Y_{0pr2}}{2} - V_{0r2}\frac{Y_{0pr2}}{2} - \left(V_{0r2} - V_{0r1\_left}\right)\frac{Y_{mpr}}{2} \tag{3.111}$$

$$A = I_{0pr2} - V_{0r2}\frac{Y_{0qr2}}{2} - \left(V_{0r2} - V_{0r1\_left}\right)\frac{Y_{mqr}}{2} \tag{3.112}$$

$$I_{0qrt} = \left(\frac{V_{0r1\_left} - V_{0r2} + Z_{0qr2}A - Z_{mqr}A}{Z_{0qr1} - Z_{mqr}}\right) \tag{3.113}$$

$$I_{0qr1} = \left(V_{0r2} - V_{0r1\_left}\right)\frac{Y_{mqr}}{2} - I_{0qrt} - V_{0r1\_left}\frac{Y_{0qr1}}{2} \tag{3.114}$$

$$I_{f0} = I_{0pr1} + I_{0qr1} \tag{3.115}$$

$$V_{0se} = V_{0r1\_left} - R_f I_{f0} \tag{3.116}$$

## 2.6 The boundary condition for various faults:

A-G fault

$$V_{1se} + V_{2se} + V_{0se} = 0 \tag{3.11}$$

B-C fault

$$V_{0se} + a^2 V_{1se} + a V_{2se} = V_{0se} + a V_{1se} + a^2 V_{2se} \quad => \quad V_{1se} = V_{2se} \tag{3.118}$$

Where $a = \angle 120°$

B-C-G fault

$$V_{0se} + a^2 V_{1se} + a V_{2se} = V_{0se} + a V_{1se} + a^2 V_{2se} = 0 \; => \; V_{1se} = V_{2se} \tag{3.119}$$

ABC fault

$$V_{1se} = 0 \tag{3.120}$$

The fault location is obtained based on $V_{1se}$, $V_{2se}$ and $V_{0se}$ and the boundary conditions. Let us take phase A to ground fault as an example:

Define:

$$f = V_{1se} + V_{2se} + V_{0se} = 0 \tag{3.121}$$

Then, we get a vector of real equations

$$F = [real(f); imag(f)]; \tag{3.122}$$

The unknown variables are $l_1$ and$R_f$. Then the Newton-Raphson method can be used to find the unknown variables. An initial value of 0.5 for $l_1$ and zero for $R_f$ can be used.

# CHAPTER FOUR

# EVALUATION STUDIES

This chapter compares the results between the Digital Distance Relaying Algorithm for First-Zone Protection for Parallel Transmission Lines with the proposed algorithm.

**1. Results of the existing algorithm for Fault location estimation of various types of faults and various fault resistances.**

The fault location for various types of faults and various fault resistances are presented in Table 4.1. The fault resistances, the estimated fault distance of each type of faults are given in column 1,2,3,4, and 5 respectively.

Table 4.1 Fault location estimation for various types of faults and various fault resistances at 50 of 300 km: (0.167 p.u.) of existing algorithm

| Fault Resistance Ω | Fault Types | | | |
|---|---|---|---|---|
| | a-g | b-c | b-c-g | a-b-c |
| 10 | 0.1668 | 0.1669 | 0.1669 | 0.1670 |
| 100 | 0.1673 | 0.1674 | 0.1674 | 0.1679 |
| 200 | 0.1678 | 0.1679 | 0.1679 | 0.1689 |

The estimated fault resistances for various types of faults and various actual fault resistances are presented in Table 4.2. The actual fault resistance is in column 1; the estimated fault resistances of each type of faults are given in column 2, 3, 4 and 5 respectively.

Table 4.2 Fault Resistances estimation for various types of faults at 50 of 300 km: (0.167 p.u.) of existing algorithm

| Actual Fault Resistance Ω | Fault Types | | | |
|---|---|---|---|---|
| | a-g | b-c | b-c-g | a-b-c |
| 10 | 9.9300 | 4.9668 | 4.9668 | 9.9429 |
| 100 | 99.2434 | 49.6793 | 49.6793 | 99.2993 |
| 200 | 198.373 | 99.2983 | 99.2983 | 198.372 |

In Table 4.3, the estimated fault location for various types of faults are presented in column 2, 3, 4, and 5.The fault resistance for each type of fault are given in the first column.

Table 4.3 Fault location estimation for various types of faults and various fault resistances at 100 of 300 km: (0.333 p.u.) of existing algorithm

| Fault Resistance Ω | Fault Types | | | |
|---|---|---|---|---|
| | a-g | b-c | b-c-g | a-b-c |
| 10 | 0.3341 | 0.3352 | 0.3352 | 0.3352 |
| 100 | 0.3347 | 0.3358 | 0.3358 | 0.3364 |
| 200 | 0.3353 | 0.3364 | 0.3364 | 0.3376 |

The fault resistance for various types of faults and various fault location are presented in Table 4.4. The actual fault resistances are in the first column, the estimated fault resistances of each type of faults are given in the second, third, fourth, and fifth column respectively.

Table 4.4 Fault Resistances estimation for various types of faults at 100 of 300 km: (0.333 p.u.) of existing algorithm

| Actual Fault Resistance Ω | Fault Types | | | |
|---|---|---|---|---|
| | a-g | b-c | b-c-g | a-b-c |
| 10 | 9.8913 | 4.9725 | 4.9725 | 9.9363 |
| 100 | 98.9859 | 49.56 | 49.56 | 99.0106 |
| 200 | 197.819 | 99.0095 | 99.0095 | 197.652 |

Table 4.5 presents the estimated fault location for various fault types and various fault resistances, various fault resistances are given in column 1. The estimated fault locations are presented in column 2, 3, 4, and 5.

Table 4.5 Fault location estimation for various types of faults and various fault resistances at 200 of 300 km: (0.667 p.u.) of existing algorithm

| Fault Resistance Ω | Fault Types | | | |
|---|---|---|---|---|
| | a-g | b-c | b-c-g | a-b-c |
| 10 | 0.6733 | 0.6810 | 0.6810 | 0.6809 |
| 100 | 0.6711 | 0.6792 | 0.6792 | 0.6774 |
| 200 | 0.6686 | 0.6774 | 0.6774 | 0.6739 |

The fault resistance for various types of faults and various fault location are presented in Table 4.6. The actual fault resistances are in the first column, the estimated fault resistances of each type of faults are given in the second, third, fourth, and fifth column respectively.

Table 4.6 Fault Resistances estimation for various types of faults at 200 of 300 km: (0.667 p.u.) of existing algorithm

| Actual Fault Resistance Ω | Fault Types | | | |
|---|---|---|---|---|
| | a-g | b-c | b-c-g | a-b-c |
| 10 | 9.7827 | 4.9458 | 4.9458 | 9.7789 |
| 100 | 99.2890 | 48.7538 | 48.7538 | 97.9493 |
| 200 | 200.164 | 97.9598 | 97.9598 | 197.900 |

Table 4.7 presents the estimated fault location for various fault types and various fault resistances, various fault resistances are given in column 1. The estimated fault locations are presented in column 2, 3, 4, and 5.

Table 4.7 Fault location estimation for various types of faults and various fault resistances at 250 of 300 km: (0.833 p.u.) of existing algorithm

| Fault Resistance Ω | Fault Types | | | |
|---|---|---|---|---|
| | a-g | b-c | b-c-g | a-b-c |
| 10 | 0.8466 | 0.8616 | 0.8616 | 0.8608 |
| 100 | 0.8379 | 0.8546 | 0.8546 | 0.8475 |
| 200 | 0.8288 | 0.8474 | 0.8474 | 0.8341 |

The fault resistance for various types of faults and various fault location are presented in Table 4.8. The actual fault resistances are in the first column, the estimated fault resistances of each type of faults are given in the second, third, fourth, and fifth column respectively.

Table 4.8 Fault Resistances estimation for various types of faults at 250 of 300 km: (0.833 p.u.) of existing algorithm

| Actual Fault Resistance Ω | Fault Types | | | |
|---|---|---|---|---|
| | a-g | b-c | b-c-g | a-b-c |
| 10 | 9.3445 | 4.4059 | 4.4059 | 8.7077 |
| 100 | 99.4489 | 44.9851 | 44.9851 | 94.1475 |
| 200 | 210.046 | 94.2177 | 94.2177 | 204.463 |

We have noticed that the error occurs when the distance and Rf is increasing.

To improve the accuracy of fault distance estimation for parallel transmission lines, we use the algorithm that we propose with the same system model that we have created earlier.

The method in estimating the fault location in long parallel transmission lines by using the equivalent PI circuit is based on a distributed parameter line model. The new method, however, assuming the local voltage and current are available, fully considers the mutual coupling impedance, the mutual coupling admittance and shunt capacitance for high precision in fault distance estimation. The following shows the results of the proposed algorithm.

**2. Results of the Proposed Algorithm with Various Types of Faults and Various Fault Resistances**.

The fault location for various types of faults and various fault resistances are presented in Table 4.9. The fault resistances, the estimated fault distance of each type of faults are given in column 1,2,3,4, and 5 respectively.

Table 4.9 Fault location estimation for various types of faults and various fault resistances at 50 of 300 km of proposed algorithm.

| Fault Resistance Ω | Fault Types | | | |
|---|---|---|---|---|
| | a-g | b-c | b-c-g | a-b-c |
| 10 | 49.9879 | 49.9957 | 49.9957 | 49.9939 |
| 100 | 49.9811 | 49.9797 | 49.9797 | 49.9554 |
| 200 | 49.9534 | 49.9576 | 49.9576 | 49.9119 |

The estimated fault resistances for various types of faults and various actual fault resistances are presented in Table 4.10. The actual fault resistance is in column 1; the estimated fault resistances of each type of faults are given in column 2, 3, 4 and 5 respectively.

Table 4.10 Fault Resistances estimation for various types of faults at 50 of 300 km of propose algorithm.

| Actual Fault Resistance Ω | Fault Types | | | |
|---|---|---|---|---|
| | a-g | b-c | b-c-g | a-b-c |
| 10 | 10.0028 | 4.9935 | 4.9935 | 10.0004 |
| 100 | 100.0144 | 50.0060 | 50.0060 | 100.020 |
| 200 | 200.0495 | 100.0198 | 100.0198 | 200.072 |

In Table 4.11, the estimated fault location for various types of faults are presented in column 2, 3, 4, and 5.The fault resistance for each type of fault are given in the first column.

Table 4.11 Fault location estimation for various types of faults and various fault resistances at 100 of 300 km:

| Fault Resistance Ω | Fault Types | | | |
|---|---|---|---|---|
| | a-g | b-c | b-c-g | a-b-c |
| 10 | 99.9732 | 99.9945 | 99.9945 | 99.9876 |
| 100 | 99.9669 | 99.9743 | 99.9743 | 99.9463 |
| 200 | 99.9368 | 99.9474 | 99.9474 | 99.8922 |

The fault resistance for various types of faults and various fault location are presented in Table 4.12. The actual fault resistances are in the first column, the estimated fault resistances of each type of faults are given in the second, third, fourth, and fifth column respectively.

Table 4.12 Fault Resistances estimation for various types of faults at 100 of 300 km:

| Actual Fault Resistance Ω | Fault Types | | | |
|---|---|---|---|---|
| | a-g | b-c | b-c-g | a-b-c |
| 10 | 9.9930 | 4.9927 | 4.9927 | 9.9999 |
| 100 | 100.0069 | 50.0071 | 50.0071 | 100.029 |
| 200 | 200.0548 | 100.0280 | 100.0280 | 200.109 |

Table 4.13 presents the estimated fault location for various fault types and various fault resistances, various fault resistances are given in column 1. The estimated fault locations are presented in column 2, 3, 4, and 5.

Table 4.13 Fault location estimation for various types of faults and various fault resistances at 200 of 300 km:

| Fault Resistance Ω | Fault Types | | | |
|---|---|---|---|---|
| | a-g | b-c | b-c-g | a-b-c |
| 10 | 199.976 | 200.0222 | 200.0222 | 200.053 |
| 100 | 200.1225 | 200.0737 | 200.0737 | 200.168 |
| 200 | 200.58 | 200.1592 | 200.1592 | 200.341 |

The fault resistance for various types of faults and various fault location are presented in Table 4.14. The actual fault resistances are in the first column, the estimated fault resistances of each type of faults are given in the second, third, fourth, and fifth column respectively.

Table 4.14 Fault Resistances estimation for various types of faults at 200 of 300 km:

| Actual Fault Resistance Ω | Fault Types | | | |
|---|---|---|---|---|
| | a-g | b-c | b-c-g | a-b-c |
| 10 | 9.9433 | 5.0021 | 5.0021 | 9.9880 |
| 100 | 99.8175 | 49.9526 | 49.9526 | 99.8153 |
| 200 | 199.4956 | 99.8258 | 99.8258 | 199.2935 |

Table 4.15 presents the estimated fault location for various fault types and various fault resistances, various fault resistances are given in column 1. The estimated fault locations are presented in column 2, 3, 4, and 5.

Table 4.15 Fault location estimation for various types of faults and various fault resistances at 250 of 300 km:

| Fault Resistance Ω | Fault Types | | | |
|---|---|---|---|---|
| | a-g | b-c | b-c-g | a-b-c |
| 10 | 249.9566 | 250.0624 | 250.0624 | 250.093 |
| 100 | 250.4679 | 250.2716 | 250.2716 | 250.630 |
| 200 | 251.0724 | 250.5968 | 250.5968 | 250.308 |

The fault resistance for various types of faults and various fault location are presented in Table 4.16. The actual fault resistances are in the first column, the estimated fault resistances of each type of faults are given in the second, third, fourth, and fifth column respectively.

Table 4.16 Fault Resistances estimation for various types of faults at 250 of 300 km:

| Actual Fault Resistance Ω | Fault Types | | | |
|---|---|---|---|---|
| | a-g | b-c | b-c-g | a-b-c |
| 10 | 9.9486 | 5.0077 | 5.0077 | 9.9732 |
| 100 | 98.9736 | 49.7108 | 49.7108 | 98.7047 |
| 200 | 195.6321 | 98.7737 | 98.7737 | 194.6927 |

### 3. Voltage and current waveforms at terminal P during fault with various types of faults

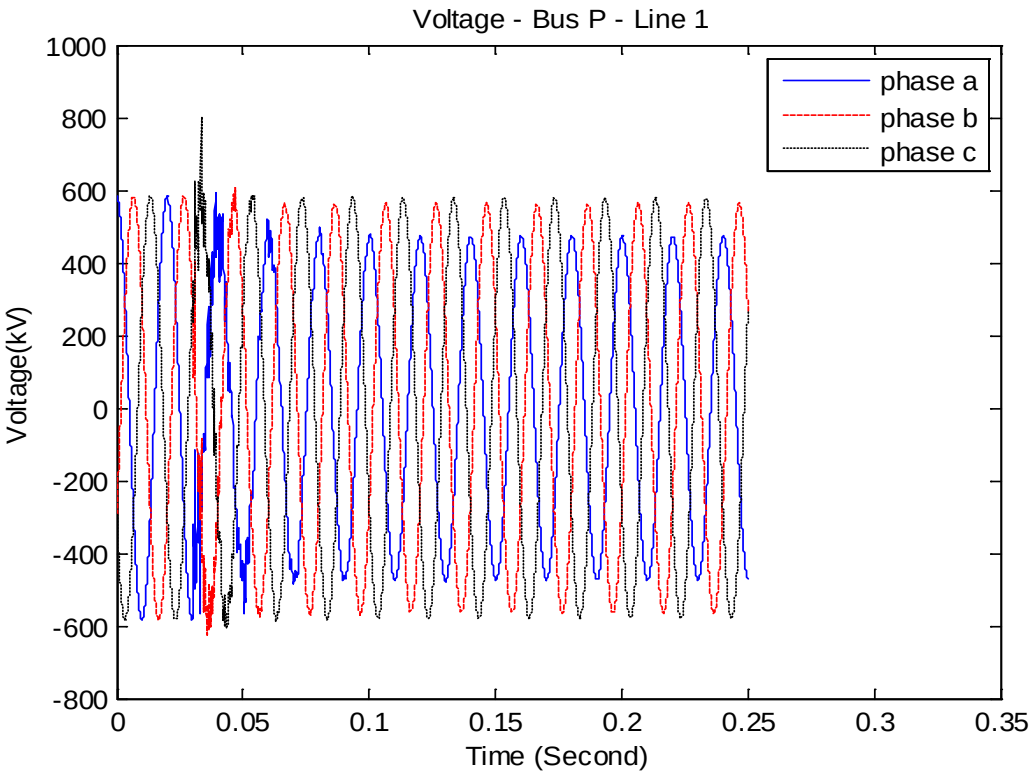


Figure 4.1.Voltage waveforms of phase a to ground fault on line 1 bus P

To show the voltage waveforms during the fault on line 1 bus P, figure 4.1 depicts the voltage waveforms of phase A-to-ground fault for the fault location at 100 km from bus P and a fault resistance of 10 Ω and the total line length between P and Q is 300 km. It can be seen that, the voltage waveforms are stable until the fault occurs at 0.0304 second then the voltage is decreasing.

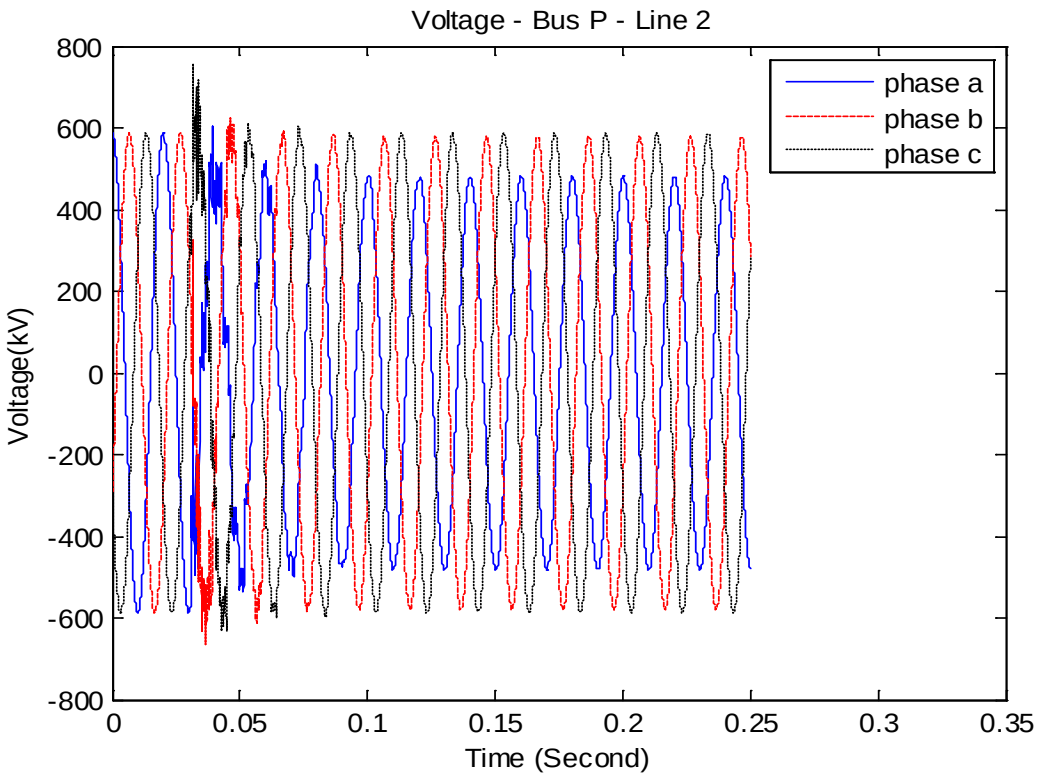


Figure 4.2.Voltage waveforms of phase a to ground fault on line 2 bus P

Figure 4.2 presents the voltage waveforms during the fault on line 2 bus P, the voltage waveforms of phase A-to-ground fault for the fault location at 100 km from bus P and a fault resistance of 10 Ω and the total line length between P and Q is 300 km. It can be seen that, the voltage waveforms are stable until the fault occurs at 0.0304 second then the voltage is decreasing.

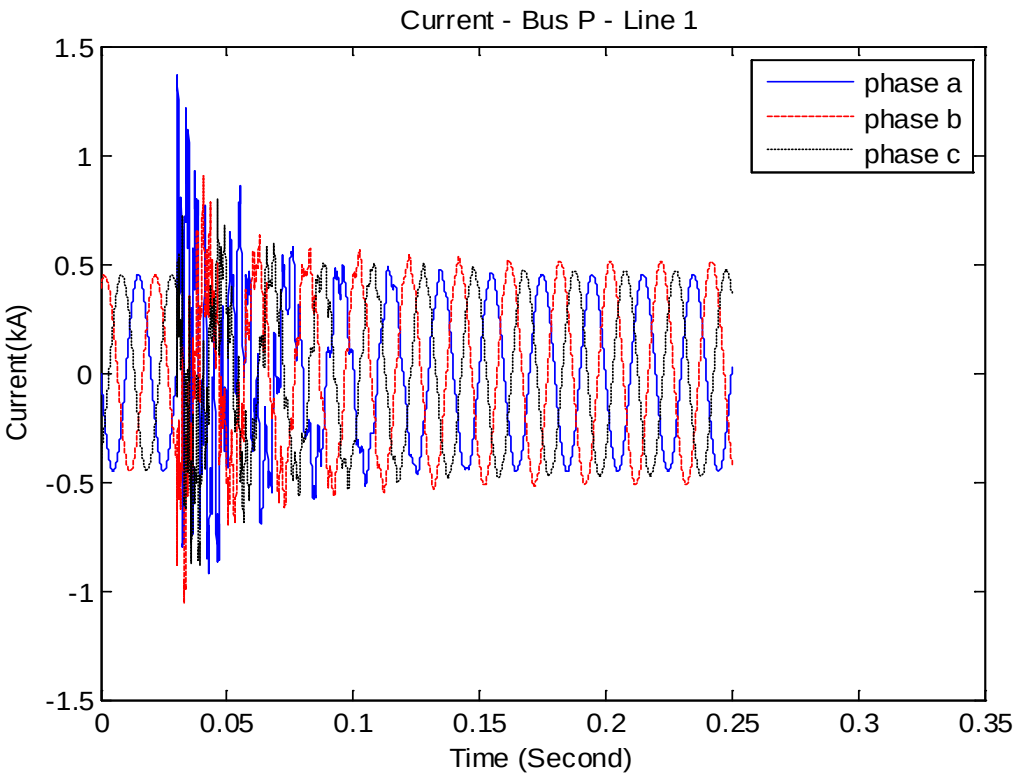


Figure 4.3.Current waveforms of phase a to ground fault on line 1 bus P

To show the current waveforms during the fault on line 1 bus P, figure 4.3 depicts the voltage waveforms of phase A-to-ground fault for the fault location at 100 km from bus P and a fault resistance of 10 Ω and the total line length between P and Q is 300 km. It can be seen that, the current waveforms are stable until the fault occurs at 0.0304 second then the current is increasing.

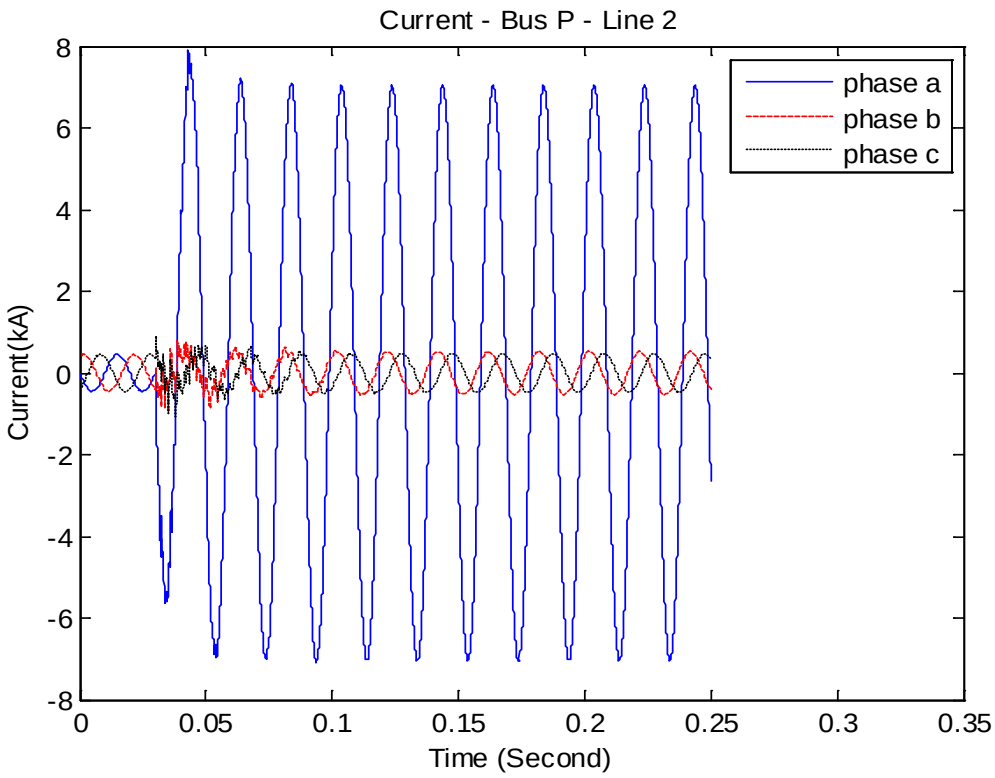


Figure 4.4.Current waveforms of phase a to ground fault on line 2 bus P

To show the current waveforms during the fault on line 2 bus P, figure 4.4 depicts the current waveforms of phase A-to-ground fault for the fault location at 100 km from bus P and a fault resistance of 10 Ω and the total line length between P and Q is 300 km. It can be seen that, the current waveforms are stable until the fault occurs at 0.0304 second then the current is increasing.

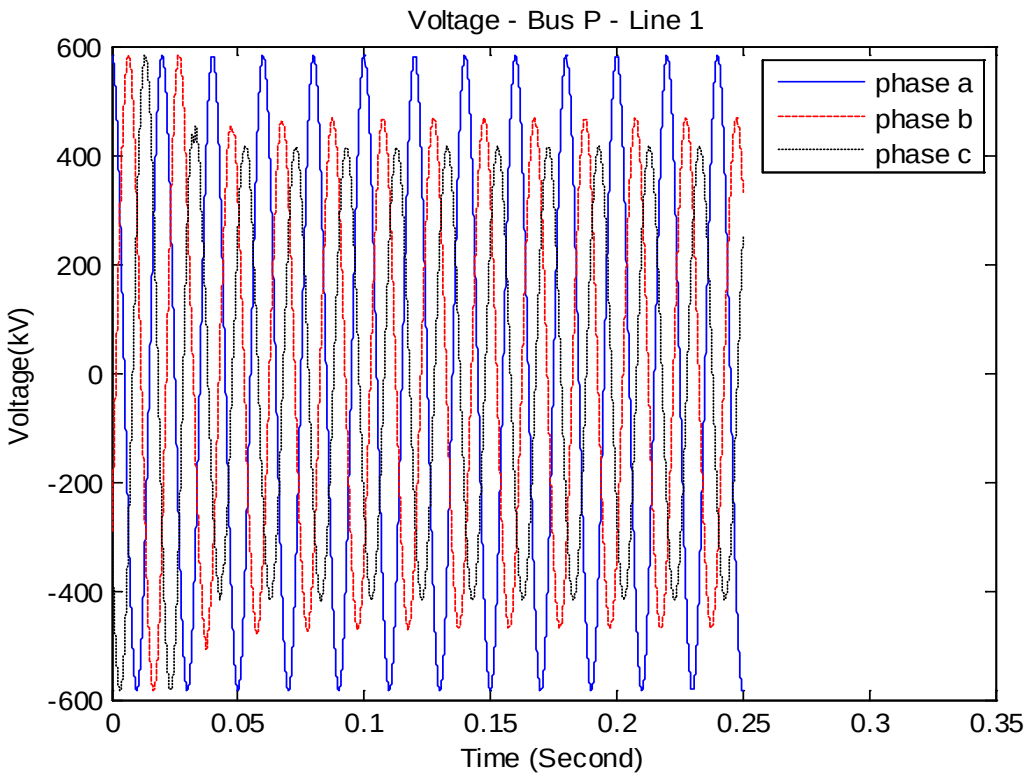


Figure 4.5. Voltage waveforms of phase b to c fault on line 1 bus P

To show the voltage waveforms during the fault on line 1 bus P, figure 4.5 depicts the voltage waveforms of phase B-to-C fault for the fault location at 100 km from bus P and a fault resistance of 10 Ω and the total line length between P and Q is 300 km. It can be seen that, the voltage waveforms are stable until the fault occurs at 0.0304 second then the voltage is decreasing.

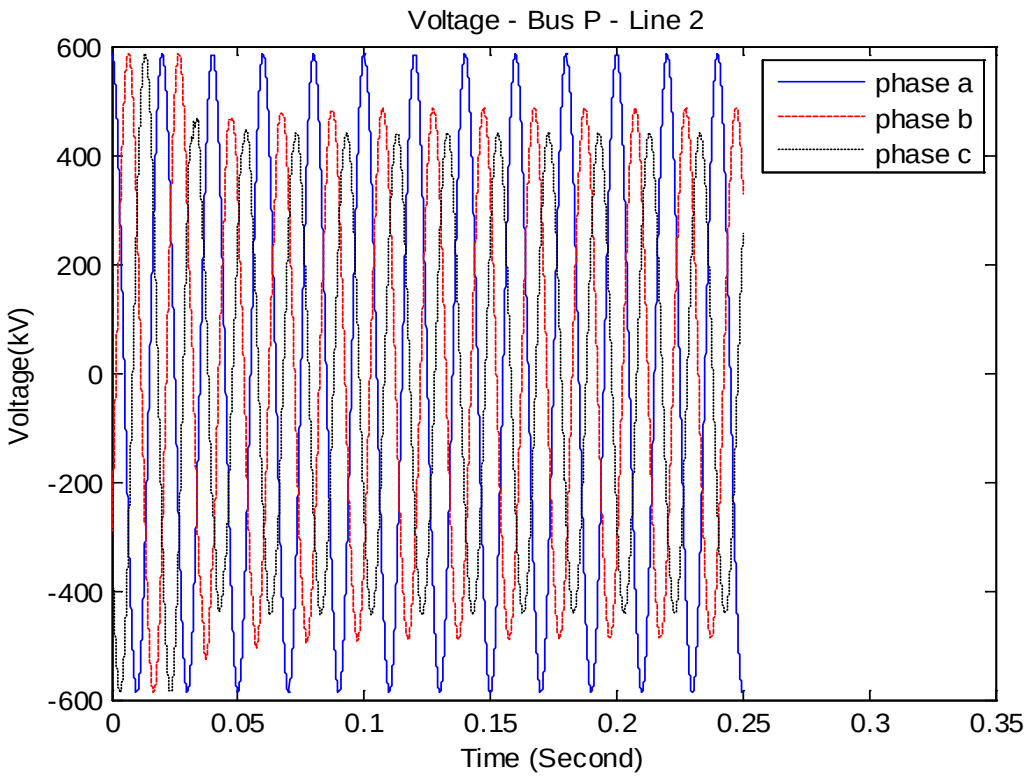


Figure 4.6. Voltage waveforms of phase b to c fault on line 2 bus P

Figure 4.6 presents the voltage waveforms during the fault on line 2 bus P, the voltage waveforms of phase B-to-C fault for the fault location at 100 km from bus P and a fault resistance of 10 Ω and the total line length between P and Q is 300 km. It can be seen that, the voltage waveforms are stable until the fault occurs at 0.0304 second then the voltage is decreasing.

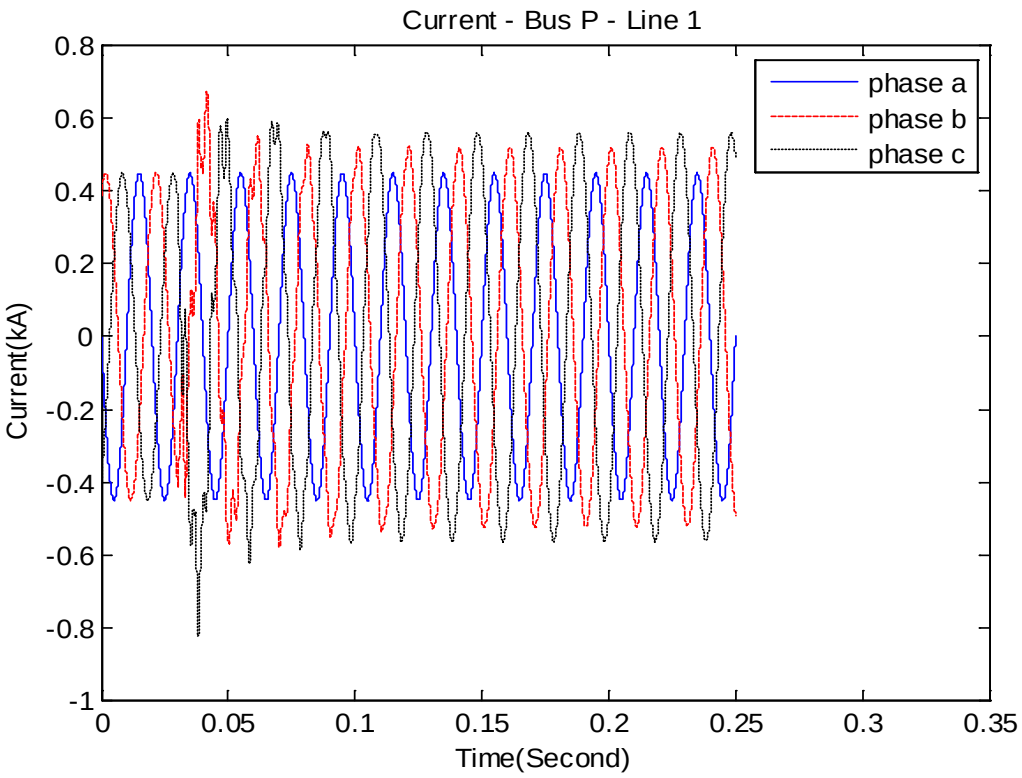


Figure 4.7. Current waveforms of phase b to c fault on line 2 bus P

To show the current waveforms during the fault on line 1 bus P, figure 4.7 depicts the current waveforms of phase B-to-C fault for the fault location at 100 km from bus P and a fault resistance of 10 Ω and the total line length between P and Q is 300 km. It can be seen that, the current waveforms are stable until the fault occurs at 0.0304 second then the current is increasing.

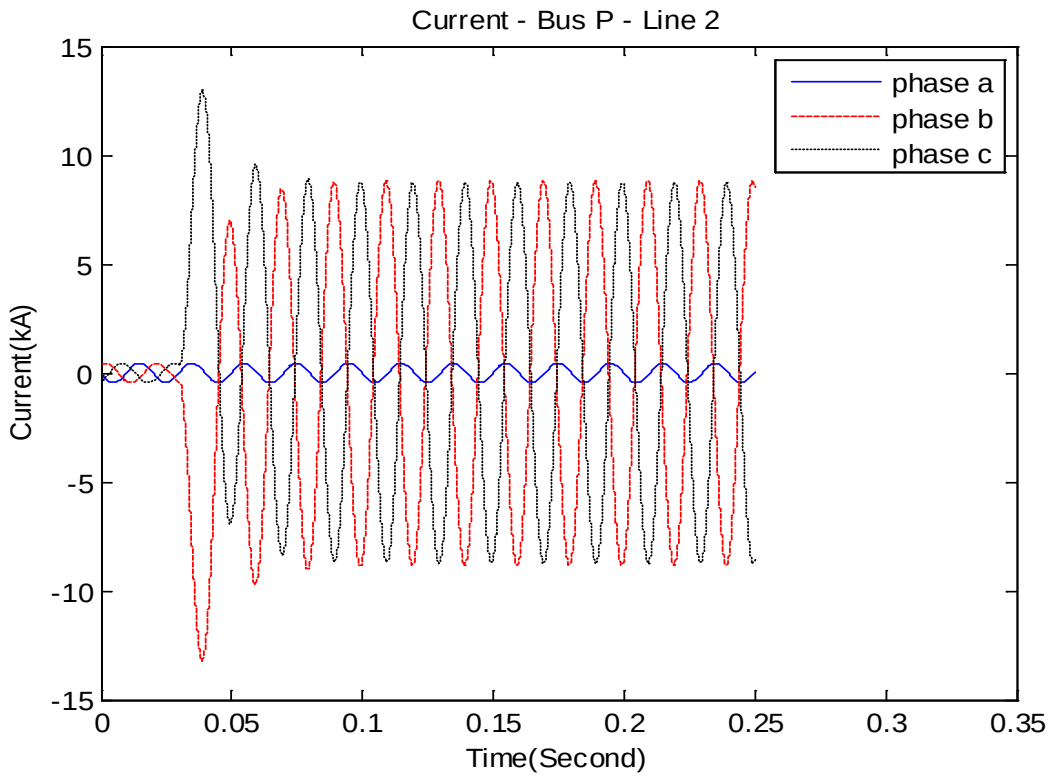


Figure 4.8.Current waveforms of phase b to c fault on line 2 bus P

Figure 4.8 presents the current waveforms during the fault on line 2 bus P, the current waveforms of phase B-to-C fault for the fault location at 100 km from bus P and a fault resistance of 10 Ω and the total line length between P and Q is 300 km. It can be seen that, the voltage waveforms are stable until the fault occurs at 0.0304 second then the current is increasing.

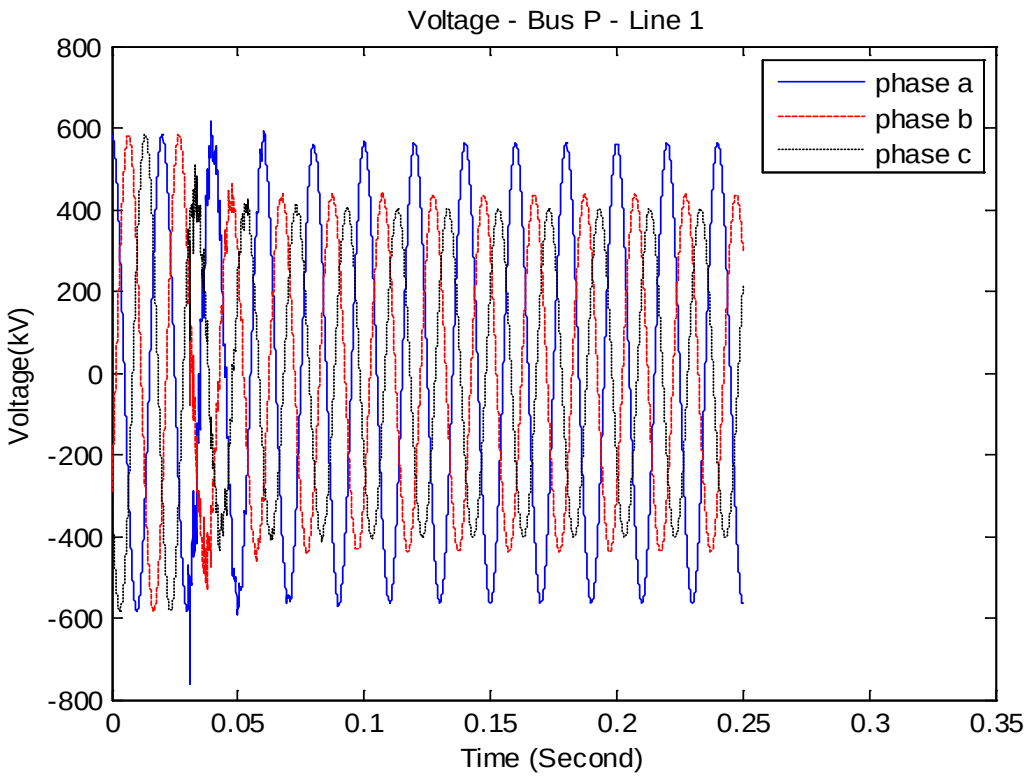


Figure 4.9.Voltage waveforms of BCG fault on line 1 bus P

To show the voltage waveforms during the fault on line 1 bus P, figure 4.9 depicts the voltage waveforms of phase B-to-C-to-ground fault for the fault location at 100 km from bus P and a fault resistance of 10 Ω and the total line length between P and Q is 300 km. It can be seen that, the voltage waveforms are stable until the fault occurs at 0.0304 second then the voltage is decreasing.

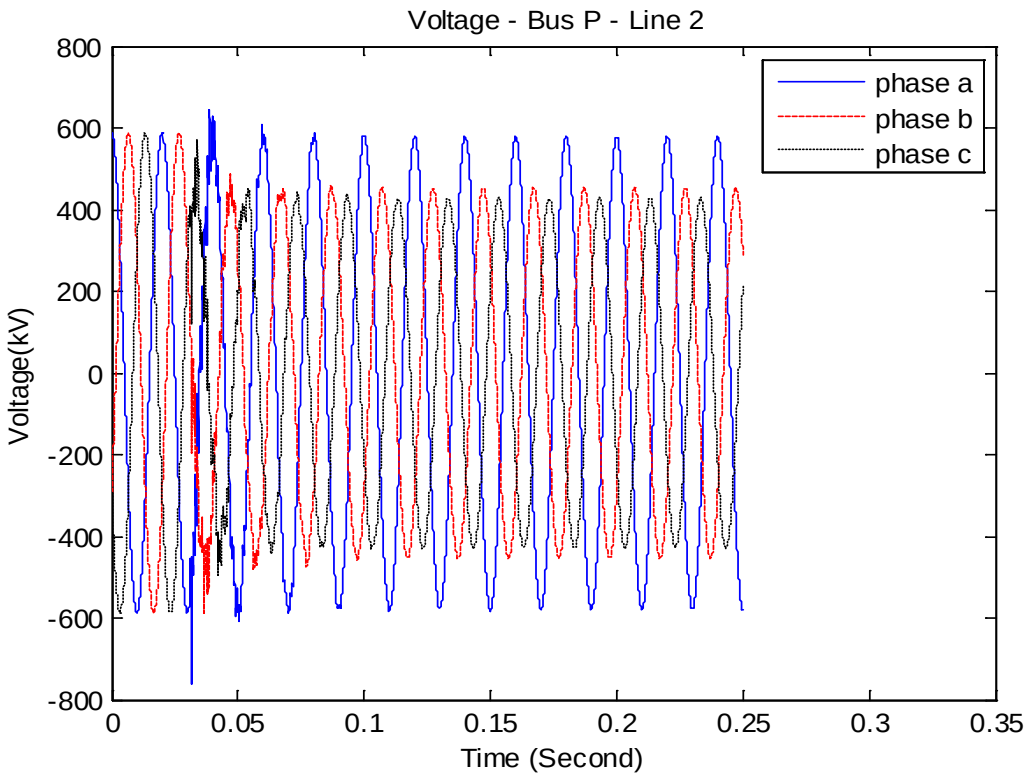


Figure 4.10.Voltage waveforms of BCG fault on line 2 bus P

To show the voltage waveforms during the fault on line 2 bus P, figure 4.10 depicts the voltage waveforms of phase B-to-C-to-ground fault for the fault location at 100 km from bus P and a fault resistance of 10 Ω and the total line length between P and Q is 300 km. It can be seen that, the voltage waveforms are stable until the fault occurs at 0.0304 second then the voltage is decreasing.

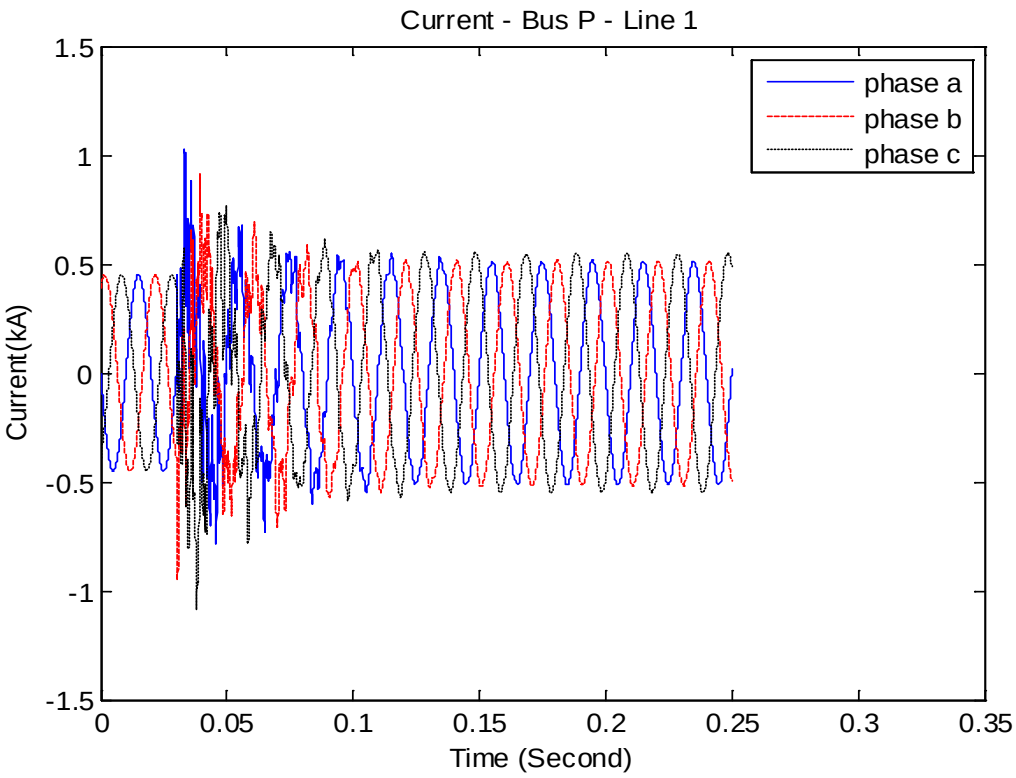


Figure 4.11.Current waveforms of BCG fault on line 1 bus P

Figure 4.11 presents the current waveforms during the fault on line 1 bus P, the current waveforms of phase B-to-C-to-ground fault for the fault location at 100 km from bus P and a fault resistance of 10 Ω and the total line length between P and Q is 300 km. It can be seen that, the voltage waveforms are stable until the fault occurs at 0.0304 second then the current is increasing.

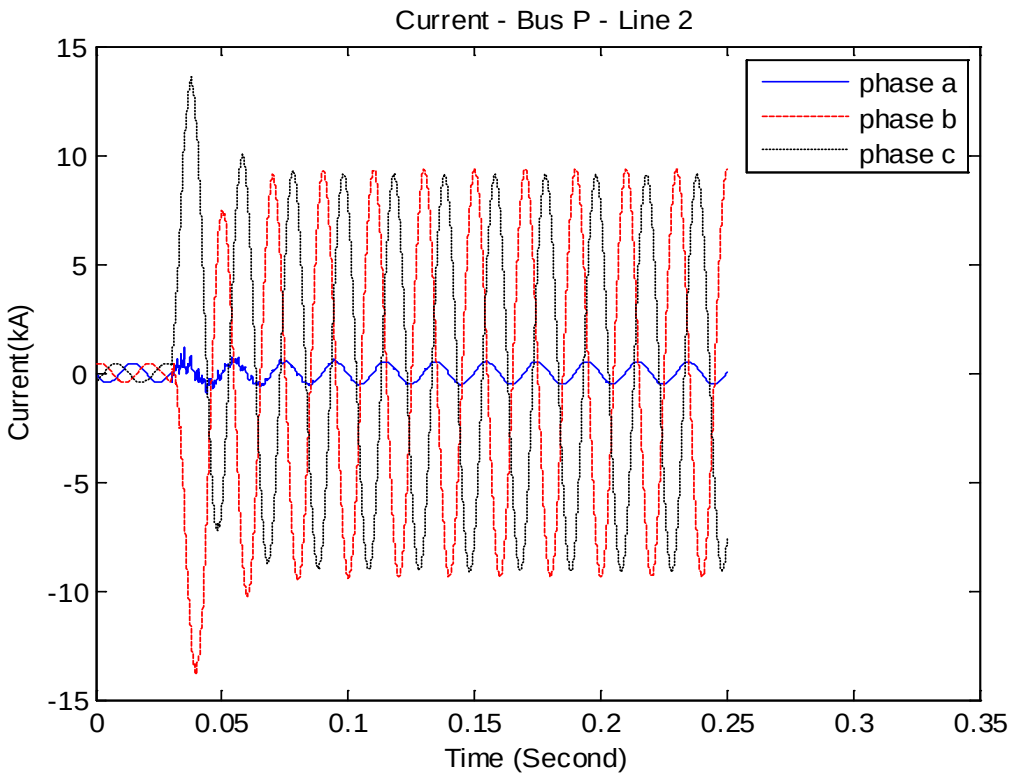


Figure 4.12. Current waveforms of BCG fault on line 2 bus P

Figure 4.12 presents the current waveforms during the fault on line 2 bus P, the current waveforms of phase B-to-C-to-ground fault for the fault location at 100 km from bus P and a fault resistance of 10 Ω and the total line length between P and Q is 300 km. It can be seen that, the voltage waveforms are stable until the fault occurs at 0.0304 second then the current is increasing.

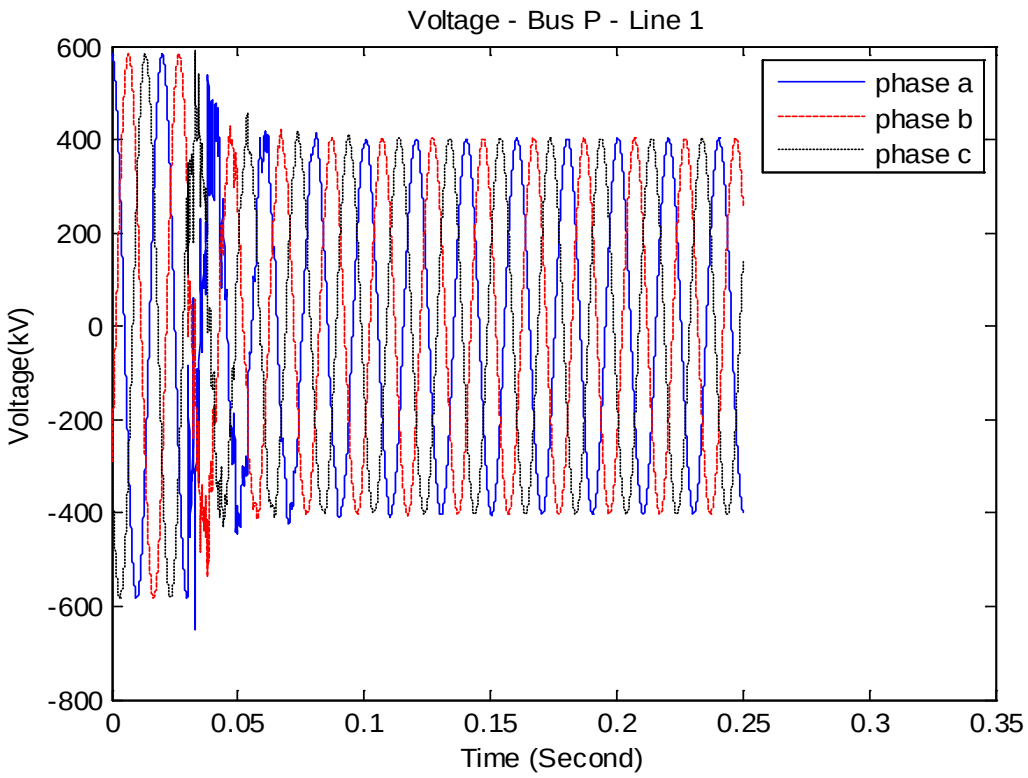


Figure 4.13. Voltage waveforms of ABC fault on line 1 bus P

To show the voltage waveforms during the fault on line 1 bus P, figure 4.13 depicts the voltage waveforms of phase A-to-B-to-C fault for the fault location at 100 km from bus P and a fault resistance of 10 Ω and the total line length between P and Q is 300 km. It can be seen that, the voltage waveforms are stable until the fault occurs at 0.0304 second then the voltage is decreasing.

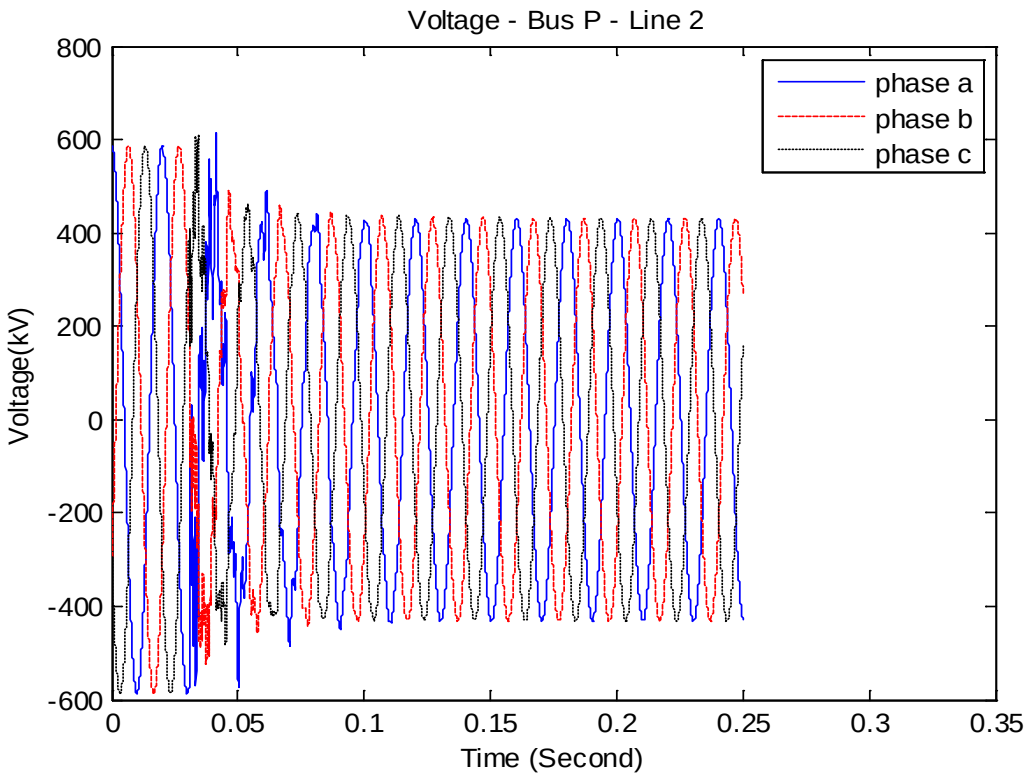


Figure 4.14.Voltage waveforms of ABC fault on line 2 bus P

To show the voltage waveforms during the fault on line 2 bus P, figure 4.14 depicts the voltage waveforms of phase A-to-B-to-C fault for the fault location at 100 km from bus P and a fault resistance of 10 Ω and the total line length between P and Q is 300 km. It can be seen that, the voltage waveforms are stable until the fault occurs at 0.0304 second then the voltage is decreasing.

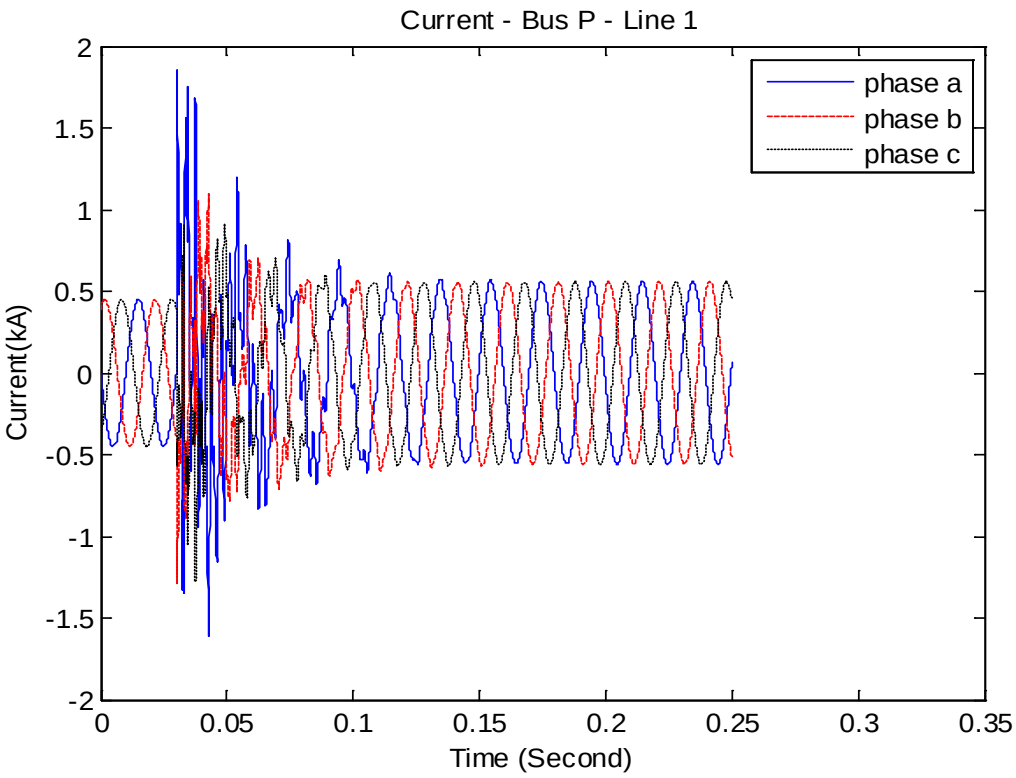


Figure 4.15.Current waveforms of ABC fault on line 1 bus P

Figure 4.15 presents the current waveforms during the fault on line 1 bus P, the current waveforms of phase A-to-B-to-C fault for the fault location at 100 km from bus P and a fault resistance of 10 Ω and the total line length between P and Q is 300 km. It can be seen that, the voltage waveforms are stable until the fault occurs at 0.0304 second then the current is increasing.

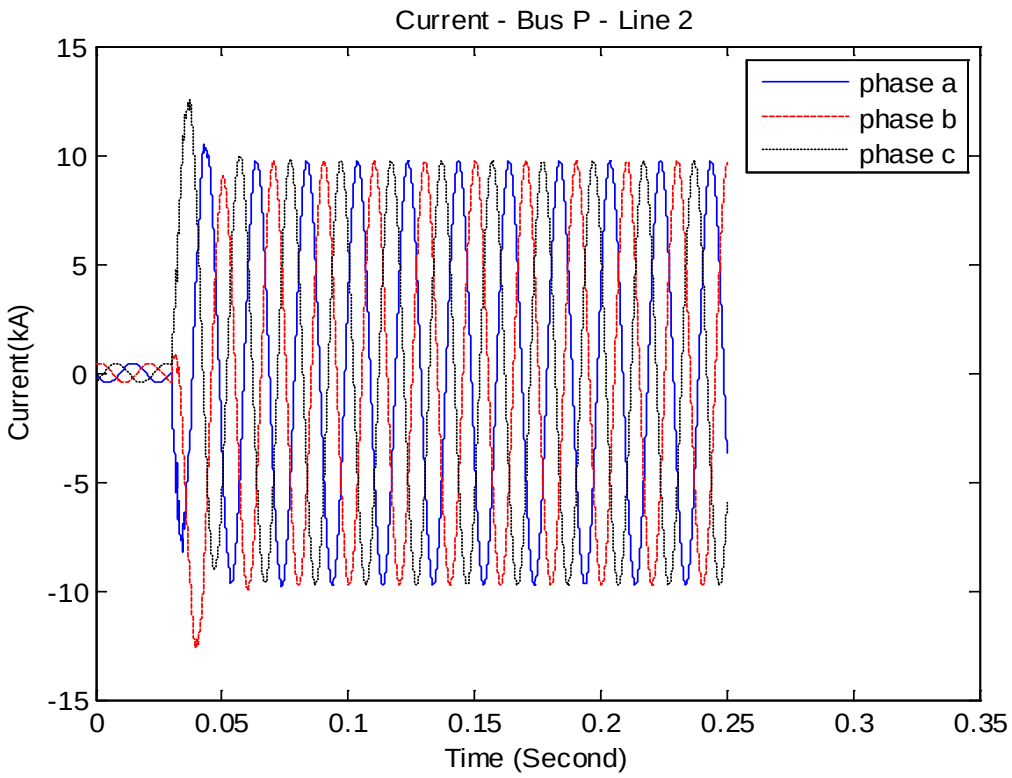


Figure 4.16.Current waveforms of ABC fault on line 2 bus P

Figure 4.16 presents the current waveforms during the fault on line 2 bus P, the current waveforms of phase A-to-B-to-C fault for the fault location at 100 km from bus P and a fault resistance of 10 Ω and the total line length between P and Q is 300 km. It can be seen that, the voltage waveforms are stable until the fault occurs at 0.0304 second then the current is increasing.

### 4. Estimated Fault Location and Fault Resistance

The proposed fault location algorithm is tested under various fault conditions and various fault types. Table 4.17 shows the estimated fault locations resulting from existing algorithm and proposed algorithm. The first column represents the fault type; the actual fault distance and actual fault resistance are in column 2 and 3. Column 4 and 5 show the estimated fault location from the existing algorithm and proposed algorithm. Column 6 and 7 show the estimated fault resistance resulting from existing algorithm and proposed algorithm respectively. It can be seen that quite close fault location estimates are produced by using the proposed algorithm and the results are quite satisfactory.

Table 4.17: Estimated fault location and fault resistance

| Fault type | Actual Fault Distance (km) | Actual Fault Resistance(ohm) | Estimated fault distance (km) | | Estimated fault resistance (ohm) | |
|---|---|---|---|---|---|---|
| | | | Existing Algorithm | Proposed Algorithm | Existing Algorithm | Proposed Algorithm |
| A-G | 50 | 10 | 50.04 | 49.9879 | 9.93 | 10.0028 |
| | | 100 | 50.19 | 49.9811 | 99.2434 | 100.0144 |
| | | 200 | 50.34 | 49.9534 | 198.3736 | 200.0495 |
| | 100 | 10 | 100.23 | 99.9732 | 9.8913 | 9.9930 |
| | | 100 | 100.41 | 99.9669 | 98.9859 | 100.0069 |

Table 4.17: Estimated fault location and fault resistance (Continued)

| Fault type | Actual Fault Distance (km) | Actual Fault Resistance(ohm) | Estimated fault distance (km) | | Estimated fault resistance (ohm) | |
|---|---|---|---|---|---|---|
| | | | Existing Algorithm | Proposed Algorithm | Existing Algorithm | Proposed Algorithm |
| | | 200 | 100.59 | 99.9368 | 197.8199 | 200.0548 |
| | 200 | 10 | 201.99 | 199.9769 | 9.7827 | 9.9433 |
| | | 100 | 201.33 | 200.1225 | 99.2890 | 99.8175 |
| | | 200 | 200.58 | 200.58 | 200.1641 | 199.4956 |
| | 250 | 10 | 253.98 | 249.9566 | 9.3445 | 9.9486 |
| | | 100 | 251.37 | 250.4649 | 99.4489 | 98.9736 |
| | | 200 | 248.64 | 251.0724 | 210.0461 | 195.6321 |
| BC | 50 | 10 [5,5] | 50.07 | 49.9957 | 4.9668 | 4.9935 |
| | | 100 [50,50] | 50.22 | 49.9797 | 49.6793 | 50.0060 |
| | | 200 [100,100] | 50.37 | 49.9576 | 99.2983 | 100.0198 |
| | 100 | 10 [5,5] | 100.56 | 99.9945 | 4.9725 | 4.9927 |
| | | 100 [50,50] | 100.74 | 99.9743 | 49.56 | 50.0071 |
| | | 200 [100,100] | 100.92 | 99.9474 | 99.0095 | 100.0280 |
| | 200 | 10 [5,5] | 204.30 | 200.0222 | 4.9458 | 5.0021 |
| | | 100 [50,50] | 203.76 | 200.0737 | 48.7538 | 49.9526 |

Table 4.17: Estimated fault location and fault resistance (Continued)

| Fault type | Actual Fault Distance (km) | Actual Fault Resistance(ohm) | Estimated fault distance (km) | | Estimated fault resistance (ohm) | |
|---|---|---|---|---|---|---|
| | | | Existing Algorithm | Proposed Algorithm | Existing Algorithm | Proposed Algorithm |
| | | 200 [100,100] | 203.22 | 200.1592 | 97.9598 | 99.8258 |
| | 250 | 10 [5,5] | 258.48 | 250.0624 | 4.4059 | 5.0077 |
| | | 100 [50,50] | 256.38 | 250.2716 | 44.9851 | 49.7108 |
| | | 200 [100,100] | 254.22 | 250.5968 | 94.2177 | 98.7737 |
| BCG | 50 | 10 [5,5] | 50.07 | 49.9957 | 4.9668 | 4.9935 |
| | | 100 [50,50] | 50.22 | 49.9797 | 49.6793 | 50.0060 |
| | | 200 [100,100] | 50.37 | 49.9576 | 99.2983 | 100.0198 |
| | 100 | 10 [5,5] | 100.56 | 99.9945 | 4.9725 | 4.9927 |
| | | 100 [50,50] | 100.74 | 99.9743 | 49.56 | 50.0071 |
| | | 200 [100,100] | 100.92 | 99.9474 | 99.0095 | 100.0280 |
| | 200 | 10 [5,5] | 204.30 | 200.0222 | 4.9458 | 5.0021 |
| | | 100 [50,50] | 203.76 | 200.0737 | 48.7538 | 49.9526 |
| | | 200 [100,100] | 203.22 | 200.1592 | 97.9598 | 99.8258 |
| | 250 | 10 [5,5] | 258.48 | 250.0624 | 4.4059 | 5.0077 |
| | | 100 [50,50] | 256.38 | 250.2716 | 44.9851 | 49.7108 |

Table 4.17: Estimated fault location and fault resistance (Continued)

| Fault type | Actual Fault Distance (km) | Actual Fault Resistance(ohm) | Estimated fault distance (km) | | Estimated fault resistance (ohm) | |
|---|---|---|---|---|---|---|
| | | | Existing Algorithm | Proposed Algorithm | Existing Algorithm | Proposed Algorithm |
| | | 200 [100,100] | 254.22 | 250.5968 | 94.2177 | 98.7737 |
| ABC | 50 | 10 | 50.10 | 49.9939 | 9.9429 | 10.0004 |
| | | 100 | 50.37 | 49.9554 | 99.2993 | 100.0208 |
| | | 200 | 50.67 | 49.9119 | 198.3727 | 200.0725 |
| | 100 | 10 | 100.56 | 99.9876 | 9.9363 | 9.9999 |
| | | 100 | 100.92 | 99.9463 | 99.0106 | 100.0290 |
| | | 200 | 101.28 | 99.8922 | 197.6526 | 200.1099 |
| | 200 | 10 | 204.27 | 200.0530 | 9.7789 | 9.9880 |
| | | 100 | 203.22 | 200.1687 | 97.9493 | 99.8153 |
| | | 200 | 202.17 | 200.3418 | 197.9007 | 199.2935 |
| | 250 | 10 | 258.24 | 250.0931 | 8.7077 | 9.9732 |
| | | 100 | 254.25 | 250.6302 | 94.1475 | 98.7047 |
| | | 200 | 250.23 | 250.3085 | 204.4630 | 194.6927 |

In this study, the fault location accuracy is measured by the percentage error calculation as

$$\%error = \frac{|Actual\ location - Estimated\ location|}{Total\ line\ length} x\ 100$$

The fault resistance estimation accuracy is measured by the percentage error calculation as

$$\%error = \frac{|Actual\ fault\ resistance - Estimated\ fault\ resistance|}{Actual\ fault\ resistance} x\ 100$$

Table 4.18 shows the percentage errors estimated fault locations resulting from existing algorithm and proposed algorithm. The first column represents the fault type; the actual fault distance and actual fault resistance are in column 2 and 3. Column 4 and 5 show the percentage errors estimated fault location from the existing algorithm and proposed algorithm. Column 6 and 7 show the percentage errors estimated fault resistance resulting from existing algorithm and proposed algorithm respectively. It can be seen that the results are in the percentage errors satisfied range by using the proposed algorithm and the results are quite satisfactory.

Table 4.18:% Error Estimated fault location and fault resistance

| Fault type | Actual Fault Distance (km) | Actual Fault Resistance(ohm) | % error Estimated fault distance (km) | | % error Estimated fault resistance (ohm) | |
|---|---|---|---|---|---|---|
| | | | Existing Algorithm | Proposed Algorithm | Existing Algorithm | Proposed Algorithm |
| A-G | 50 | 10 | 0.1333 | 0.004033 | 0.7 | 0.028 |
| | | 100 | 0.06333 | 0.0063 | 0.7566 | 0.0144 |
| | | 200 | 0.11333 | 0.015533 | 0.8132 | 0.02475 |
| | 100 | 10 | 0.07667 | 0.008933 | 1.087 | 0.07 |
| | | 100 | 0.13667 | 0.011033 | 1.0141 | 0.0069 |
| | | 200 | 0.19667 | 0.021067 | 1.09005 | 0.0274 |
| | 200 | 10 | 0.66333 | 0.0077 | 2.173 | 0.567 |
| | | 100 | 0.44333 | 0.04083 | 0.711 | 0.1825 |
| | | 200 | 0.19333 | 0.19333 | 0.08205 | 0.2522 |
| | 250 | 10 | 1.32667 | 0.014467 | 6.555 | 0.514 |
| | | 100 | 0.45667 | 0.15497 | 0.5511 | 1.0264 |
| | | 200 | 0.453333 | 0.35747 | 5.02305 | 2.18395 |
| BC | 50 | 10 [5,5] | 0.02333 | 0.001433 | 0.664 | 0.13 |
| | | 100 [50,50] | 0.07333 | 0.006767 | 0.6414 | 0.012 |

Table 4.18:% Error Estimated fault location and fault resistance (Continued)

| Fault type | Actual Fault Distance (km) | Actual Fault Resistance(ohm) | % error Estimated fault distance (km) | | % error Estimated fault resistance (ohm) | |
|---|---|---|---|---|---|---|
| | | | Existing Algorithm | Proposed Algorithm | Existing Algorithm | Proposed Algorithm |
| | | 200 [100,100] | 0.12333 | 0.014133 | 0.7017 | 0.0198 |
| | 100 | 10 [5,5] | 0.18667 | 0.001833 | 0.55 | 0.146 |
| | | 100 [50,50] | 0.24667 | 0.008567 | 0.88 | 0.0142 |
| | | 200 [100,100] | 0.30667 | 0.017533 | 0.9905 | 0.028 |
| | 200 | 10 [5,5] | 1.43333 | 0.0074 | 1.084 | 0.042 |
| | | 100 [50,50] | 1.25333 | 0.02457 | 2.4924 | 0.0948 |
| | | 200 [100,100] | 1.07333 | 0.05307 | 2.0402 | 0.1742 |
| | 250 | 10 [5,5] | 2.82667 | 0.0208 | 11.882 | 0.154 |
| | | 100 [50,50] | 2.12667 | 0.09053 | 10.0298 | 0.5784 |
| | | 200 [100,100] | 1.40667 | 0.19893 | 5.7823 | 1.2263 |
| BCG | 50 | 10 [5,5] | 0.02333 | 0.001433 | 0.664 | 0.13 |
| | | 100 [50,50] | 0.07333 | 0.006767 | 0.6414 | 0.012 |
| | | 200 [100,100] | 0.12333 | 0.014133 | 0.7017 | 0.0198 |
| | 100 | 10 [5,5] | 0.18667 | 0.001833 | 0.55 | 0.146 |

Table 4.18:% Error Estimated fault location and fault resistance (Continued)

| Fault type | Actual Fault Distance (km) | Actual Fault Resistance(ohm) | % error Estimated fault distance (km) | | % error Estimated fault resistance (ohm) | |
|---|---|---|---|---|---|---|
| | | | Existing Algorithm | Proposed Algorithm | Existing Algorithm | Proposed Algorithm |
| | | 100 [50,50] | 0.24667 | 0.008567 | 0.88 | 0.0142 |
| | | 200 [100,100] | 0.30667 | 0.017533 | 0.9905 | 0.028 |
| | 200 | 10 [5,5] | 1.43333 | 0.0074 | 1.084 | 0.042 |
| | | 100 [50,50] | 1.25333 | 0.02457 | 2.4924 | 0.0948 |
| | | 200 [100,100] | 1.07333 | 0.05307 | 2.0402 | 0.1742 |
| | 250 | 10 [5,5] | 2.82667 | 0.0208 | 11.882 | 0.154 |
| | | 100 [50,50] | 2.12667 | 0.09053 | 10.0298 | 0.5784 |
| | | 200 [100,100] | 1.40667 | 0.19893 | 5.7823 | 1.2263 |
| ABC | 50 | 10 | 0.03333 | 0.002033 | 0.571 | 0.004 |
| | | 100 | 0.12333 | 0.014867 | 0.7007 | 0.0208 |
| | | 200 | 0.22333 | 0.029367 | 0.81365 | 0.03625 |
| | 100 | 10 | 0.18667 | 0.004133 | 0.637 | 0.001 |
| | | 100 | 0.30667 | 0.0179 | 0.9894 | 0.029 |
| | | 200 | 0.42667 | 0.035933 | 1.1737 | 0.05495 |
| | 200 | 10 | 1.42333 | 0.01767 | 2.211 | 0.12 |

Table 4.18:% Error Estimated fault location and fault resistance (Continued)

| Fault type | Actual Fault Distance (km) | Actual Fault Resistance(ohm) | % error Estimated fault distance (km) | | % error Estimated fault resistance (ohm) | |
|---|---|---|---|---|---|---|
| | | | Existing Algorithm | Proposed Algorithm | Existing Algorithm | Proposed Algorithm |
| | | 100 | 1.07333 | 0.05623 | 2.0507 | 0.1847 |
| | | 200 | 0.72333 | 0.11393 | 1.04965 | 0.35325 |
| | 250 | 10 | 2.74667 | 0.03103 | 12.923 | 0.268 |
| | | 100 | 1.41667 | 0.21007 | 5.8525 | 1.2953 |
| | | 200 | 0.07667 | 0.10283 | 2.2315 | 2.65365 |

# CHAPTER FIVE

# CONCLUSION

Fault that occurs on a power transmission line can prolong the outage time if the fault location is not located as quickly as possible. The faster the fault location is found, the sooner the system can be restored and outage time can be reduced.

This research develops a new accurate algorithm for parallel transmission lines, taking into consideration mutual coupling impedance, mutual coupling admittance, and shunt capacitance. The equivalent PI circuit based on a distributed parameter line model for positive, negative, and zero sequence networks have been constructed for system analysis during the fault.

Evaluation studies have been carried out to verify the proposed method. Comparing the results obtained by the existing algorithm and the proposed algorithm, it is evinced that the developed algorithm can achieve highly accurate estimates and is promising for practical applications.

Being able to pinpoint the fault location more accurately will help reduce outage time, save money, and improve system reliability.

## BIBLIOGRAPHY

[1] WHEELER, S.A.: 'Influence of Mutual Coupling between Parallel Circuits on the Setting of Distance Protection', Proc. IEE, 1970, 117, (2), pp. 439-444.

[2] Y. Liao, S. Elangovan, "Digital Distance Relaying Algorithm for First-Zone Protection for Parallel Transmission Lines," Proc.-Gener. Transm. Distrib. IEE, 1998, 145, (5), pp. .531-536.

[3] L. Eriksson, M. M. Saha and G. D. Rockfeller, "An accurate fault location with compensation for apparent reactance in the fault resistance resulting from remote-end infeed", IEEE Trans., vol. PAS-104, no. 2, pp. 424-436, Feb. 1985.

[4] Y. Hu, D. Novosel, M. M. Saha, " An Adaptive Scheme for Parallel-Line Distance Protection," IEEE Trans. Power Delivery, vol.17, pp. 105-110, January 2002.

[5] J. Izykowski, E. Rosolowski and M. Mohan Saha, "Locating faults in parallel transmission lines under availability of complete measurements at one end", in IEE Proceedings- Generation, Transmission and Distribution, vol. 145, no. 2, March 2, 2004, pp. 268-273.

[6] A. Wiszniewski, "Accurate fault impedance locating algorithm,", IEE Proc. C, Gener. Transm. Distrib., 1983, 130, (6), pp.311-314.

[7] Zhang, Q., Zhang, Y., Song, W., and Yu, Y.: 'Transmission line fault location for phase-to-earth fault using one-terminal data', IEE Proc. Gener. Transm. Distrib., 1999,146, (2), pp.121-124.

[8] D. Novosel, D. G. Hart, E. Udren, and J. Garitty, " Unsynchronised two-terminal fault location estimation," IEEE Trans. Power Del., vol. 11, no. 1, pp. 130-138, Jan 1996.

[9] M.I. Gilany, O.P. Malik, and G.S. Hope.: 'A digital protection technique for parallel transmission lines using a single relay at each end', IEEE Trans. Power Deliv., 1992, 7, (1), pp.118-123

[10] M.M. Eissa, and M. Masoud.: 'A novel digital distance relaying technique for transmission line protection', IEEE Trans. Power Deliv., 2001, 16, (3), pp.380-384.

[11] Maheshwari, R.P., Bhalja. B.: ' Protection of double-circuit line using wavelet transform', Journal of the Institution of Engineers(India): Electrical Engineering Division, v 87, n SEPT, Sept 28,2006, pp. 67-70.

[12] Bhalja. Bhavesh R., Maheshwari. Rudra Prakash,: 'High-resistance faults on two terminal parallel transmission line: Analysis, simulation studies, and an adaptive distance relaying scheme', IEEE Trans. Power Deliv.,2007, v22, n2, pp. 801-812.

[13] Mukerjee. R.N, Bin Abdullah, Mohd Faris, Tan. K.K and Nallagownden. Perumal.:' Acoiding under-reaching in twin circuit lines without residual current input from the parallel line', 8th International power engineering conference, IPEC 2007, 2007, pp.1115-1120.

[14] Kawecki. R. and Izykowski. J.: 'Locating faults in parallel transmission lines under lack of measurements from the healthy line circuit', Proceedings of the

Universities Power Engineering Conference, v36 UPEC 2001, 36th Universities Power Engineering Conference, 2001, p 1635-1639.

[15] Y. Liao, “Fault location utilizing unsynchronized voltage measurements during fault,” Elect. Power Components Syst., vol. 34, no. 12, pp.1283-1293, Dec. 2006.

[16] Y. Liao, M. Kezunovic, “Optimal Estimate of Transmission Line Fault Location Considering Measurment Errors,” IEEE Trans. Power Delivery, vol. 22, No. 3, July 2007.

[17] Y. Liao, “Equivalent PI Circuit For Zero-Sequence Networks Of Parallel Transmission Lines,” Electric Power Components and Systems.

[18]John Grainger and William Stevenson, Power System Analysis, McGraw-Hill, Inc., NY, USA, 1994.

[19] S. H. Horowiz, A. G. Phadke, and J. S. Thorp, “Adaptive transmission system relaying,” IEEE Trans. Power Delivery, vol. 3, pp. 1436-1445, Oct. 1988.

[20] G. D. Rockefeller, C. L. Wagner, J. R. Linders, K. L. Hicks, and D. T. Rizy, “Adaptive transmission system relaying concepts for improved performance,” IEEE Trans. Power Delivery, vol. 3, pp.1446-1458, Oct. 1988.

[21] J. Lewis Blackburn, Protective Relaying Principles and Applications, Second Edition, Marcel Dekker, New York, 1998.

[22] A.G. Jongepier and L. van der Sluis, “Adaptive Distance Protection of a Double-Circuit Line,” IEEE Trans. Power Delivery, vol.9, pp. 1289-1295, July 1994.

[23] A.K. Jampala, S.S Venkata, M.J. Damborg, “Adaptive Transmission Protection : Concepts and Computational Issues”, IEEE Trans. Power Delivery, vol. 4, pp.177-185, No. 1 , January 1989.

[24] Y. Hu, D. Novosel, M.M. Saha, Volker Leitloff, “Improving Parallel Line Distance Protection With Adaptive Techniques” IEEE Trans. Power Delivery, 2000.

[25] Y. Liao, “Unsynchronized fault location based on distribute parameter line model”, Electric Power Components & System, vol. 35, No. 9, 2007 pp.1061-1077.

[26] Tamer Kawady and Jurgen Stenzel, “A practical Fault Location Approach for Double Circuit Transmission Lines Using Single End Data”, IEEE Transactions on Power Delivery, Vol. 18, pp.1166-1173, No. 4, October 2003.

## VITA

Born in 1964 in Khonkaen, Thailand

Education:

University of Kentucky, Master of Science in Electrical Engineering, 2005-2007

University of Kentucky, Bachelor of Science in Electrical Engineering, 2002-2004

Pramote Chaiwan